

Algebraic Wasserstein distances and stable homological invariants of data

Jens Agerberg Andrea Guidolin Isaac Ren Martina Scolamiero

Abstract

Distances have a ubiquitous role in persistent homology, from the direct comparison of homological representations of data to the definition and optimization of invariants. In this article we introduce a family of parametrized pseudometrics between persistence modules based on the algebraic Wasserstein distance defined by Skraba and Turner, and phrase them in the formalism of noise systems. This is achieved by comparing p -norms of cokernels (resp. kernels) of monomorphisms (resp. epimorphisms) between persistence modules and corresponding bar-to-bar morphisms, a novel notion that allows us to bridge between algebraic and combinatorial aspects of persistence modules. We use algebraic Wasserstein distances to define invariants, called Wasserstein stable ranks, which are 1-Lipschitz stable with respect to such pseudometrics. We prove a low-rank approximation result for persistence modules which allows us to efficiently compute Wasserstein stable ranks, and we propose an efficient algorithm to compute the interleaving distance between them. Importantly, Wasserstein stable ranks depend on interpretable parameters which can be learnt in a machine learning context. Experimental results illustrate the use of Wasserstein stable ranks on real and artificial data and highlight how such pseudometrics could be useful in data analysis tasks.

MSC: 55N31, 62R40, 55U99

Keywords: Persistent homology, persistence modules, stable topological invariants of data, Wasserstein metrics

Contents

1	Introduction	2
2	Preliminaries	5
2.1	Persistence modules and persistent homology	5
2.2	Contours	7
2.3	Noise systems	8
2.4	Pseudometrics between persistence modules	9
2.5	Hierarchical stabilization and stable rank	9
2.6	p -norms	10
3	Monomorphisms, epimorphisms, and their p-norms	11
3.1	Free presentations of monomorphisms	11
3.2	Finding monomorphisms with smaller cokernels	12

3.3	Bar-to-bar epimorphisms	20
3.4	Comparing bar-to-bar morphisms with induced matchings	22
4	Noise systems and Wasserstein pseudometrics	24
4.1	Pseudometrics associated to noise systems	24
4.2	p -norms of persistence modules and contours	26
4.3	Contours and algebraic Wasserstein distances	30
4.4	Algebraic and combinatorial (p, C) -Wasserstein distances	31
4.5	Algebraic parametrized Wasserstein distances	33
5	Wasserstein stable ranks: computations and stability	38
5.1	Computation of the stable rank with Wasserstein distances	38
5.2	Interleaving distance between stable ranks	40
5.3	Metric learning	43
6	Examples of analyses with Wasserstein stable ranks	43
6.1	Synthetic data	44
6.2	Brain artery data	47

1 Introduction

While Topological Data Analysis (TDA) has historically focused on studying the global shape of data, persistent homology has since grown to provide popular techniques for incorporating both global topological features and local geometry into data analysis pipelines [AM21]. Through the lens of persistent homology, global topological features can be encoded by long bars in a barcode decomposition of the persistence module, while local geometric features are characterized by short bars in the barcode. Indeed, both the information of long bars and short bars in the barcode [BMM⁺16, HNH⁺16], as well as their location along the filtration scale [SHP17, CR20, ARSC21], turn out to be relevant in data analysis tasks. Wasserstein distances offer a way to determine a trade-off between global and local features in persistence. Such distances, first introduced in [CSEHM10] in the context of persistent homology, have been widely used in applications and have been studied both from a combinatorial perspective and more recently with an algebraic approach [BSS23, ST20]. Wasserstein distances are parametrized by two parameters in $[1, \infty]$ commonly fixed to the values of 1, 2 and ∞ . One of the aims of this article is to define a richer family of parametrized Wasserstein distances where, in addition to standard parameters determining sensitivity to short bars globally in the parameter space, a *contour* is introduced to locally weight different parts of the parameter space. We propose that the optimal parameter values for a particular task should be learned in a machine learning context. Our contribution is part of more general efforts of identifying parametrized families of metrics and invariants for persistence [BDSS15, SCL⁺17, HKNU17, ZW19, CCI⁺20].

Algebraic Wasserstein distances. Our parametrized Wasserstein distances are defined algebraically, as a generalization of the *algebraic Wasserstein distances*, associated with p -norms of persistence modules, defined in [ST20]. The study of algebraic distances between persistence

modules is an active research direction in TDA, as demonstrated by the recent works on amplitudes [GNOW21] and exact weights [BSS23]. In this article we provide an algebraic proof that the p -norm defines a pseudometric on persistence modules. Our algebraic proof is based on the framework of noise systems introduced in [SCL⁺17], where it is shown that if a family of subsets of persistence modules, parametrized by $[0, \infty)$, follows the noise systems axioms then an associated pseudometric can be constructed. This approach is different from the one presented in [ST20] where a correspondence between the pseudometric induced by the p -norm and the Wasserstein distance between persistence diagrams is constructed to prove that such a norm defines a pseudometric on persistence modules. The axioms of noise systems are proved as a consequence, using the triangular inequality. We see an advantage in the algebraic approach because it can be easily generalized to define more pseudometrics on persistence modules, as for example the distances $d_{S^p, C}^q$ we introduce by combining contours and p -norms, which at the combinatorial level were not known. Furthermore the noise system framework [SCL⁺17] shows that among the five algebraic conditions presented in [ST20, Sect. 7.3] to define a pseudometric starting from a norm, only three are necessary. Proving the axioms of noise systems for the p -norm allows us to understand how this norm interacts with monomorphisms, epimorphism and short exact sequences, shedding more light on this norm on persistence modules. It is interesting to see that Wasserstein pseudometrics fit in the noise system framework, as they are fundamentally different from noise systems that have been studied from a computational perspective so far. In fact, algorithms for the computation of stable ranks (that can be seen as vectorizations of persistence modules depending on the noise system) were only developed for so-called *simple noise systems* [GC17, CR20]. These noise systems have the extra property of being closed under direct sums, and can intuitively be thought of as being sensitive only to the longest bars, which leads to L^∞ type distances. Algebraic Wasserstein distances for $p < \infty$ are of a different nature, in particular they are not closed under direct sums. From a practical and computational perspective, combinatorial distances between persistence diagrams are more straightforward to compute than algebraic distances between persistence modules. The combinatorial (p, C) -Wasserstein distances associated to $d_{S^p, C}^p$ in Section 4.4 offer a convenient way to compute contour distances and the combination of contour and Wasserstein distances between persistence modules, relying on the already developed computational machinery for Bottleneck ($p = \infty$) and Wasserstein distances between persistence diagrams. In this article, however, our focus is not on the computation of the Wasserstein distance between two given persistence modules, but on invariants called Wasserstein stable ranks defined and computed using the distances.

Bar-to-bar morphisms. The approach carried out in this article for proving that p -norms of persistence modules satisfy the axioms of noise systems relies on comparing monomorphisms (resp. epimorphisms) between persistence modules and so-called *bar-to-bar* monomorphisms (resp. epimorphisms) between the same persistence modules. Intuitively, in a bar-to-bar morphism (see Definition 3.1) every bar in the barcode decomposition of the domain maps non-trivially to at most one bar in the barcode decomposition of the codomain. Bar-to-bar morphisms are thus much simpler than general morphisms of persistence modules, and we show that they can be used to effectively reduce algebraic problems to easier problems of combinatorial na-

ture. In particular, an important problem related to the definition and construction of algebraic distances is the minimization of kernels and cokernels of morphisms (see e.g. Definition 4.3) with respect to a chosen notion of “size”, which in this article is the p -norm of persistence modules (Section 2.6) or a more general notion of norm combining p -norms and contours (Definition 4.7). Our main theoretical results Theorem 3.14 and Theorem 3.16 state that for any monomorphism (resp. epimorphism) between two persistence modules there exists a bar-to-bar monomorphism (resp. epimorphism) between the same persistence modules whose cokernel (resp. kernel) has smaller or equal norm.

Bar-to-bar monomorphisms and epimorphisms are fundamentally different from the induced matchings introduced in [BL15], and thus from other notions defined using the induced matchings, like the sub-barcode matchings of [CGS22]. However, in Section 3.4 we use bar-to-bar morphisms to prove that, given any monomorphism (resp. epimorphism) of persistence modules, the induced matching provides a way to construct another monomorphism (resp. epimorphism) between the same modules whose cokernel (resp. kernel) has minimal norm (Corollary 3.20 and Corollary 3.22). Several other key results of this article are proven leveraging Theorem 3.14 and Theorem 3.16. For example, we use these theorems to show that p -norms of persistence modules satisfy a key axiom of noise systems (Lemma 4.15), providing a proof that is fundamentally different from the one in [ST20] as it is carried out entirely at an algebraic level and does not rely on the Wasserstein distances between persistence diagrams. We use our main results of Section 3 also to prove a low-rank approximation result for persistence modules, analogous for example to the Eckart-Young-Mirsky theorem in the context of matrices (compare e.g. with [GHS87, Sect. 1] and references therein), where the notion of rank we use for persistence modules is the number of bars in the barcode decomposition. Given a persistence module X of rank k , for every $r \leq k$ we identify a persistence module of rank r that is closest to X in algebraic Wasserstein distance, and we express its distance from X (Proposition 4.30 and Proposition 4.32). These results and their generalization (Proposition 4.32) allow us to compute Wasserstein stable ranks (see Proposition 5.3), the invariants that we introduce in this article.

Wasserstein stable ranks. The computation of Wasserstein distances between persistence modules remains expensive despite recent progress [KMN17], and the space of persistent modules is not directly amenable to statistical methods and machine learning. For these reasons, feature maps from persistence modules or diagrams have become an important component of the TDA machine learning pipeline. These techniques introduce a map between the space of persistence modules and a vector space where statistical and machine learning methods are well-developed. We propose a new class of feature maps, directly related to the Wasserstein distances $d_{Sp,C}^q$ between persistence modules and with interpretable, learnable parameters. Having fixed a pseudometric in the family of Wasserstein distances $d_{Sp,C}^q$, the Wasserstein stable rank of a persistence module with respect to the chosen pseudometric can be explicitly computed with a formula (Proposition 5.3) we derived from our results on monomorphisms and epimorphisms. The computational complexity of determining the Wasserstein stable rank is $O(n \log n)$ in the number n of bars of a persistence module.

A parametrized family of stable ranks can be obtained by varying the Wasserstein distances, opening up for the possibility to tune parameters for a particular task, resulting in feature maps

that focus on the discriminative aspects of the persistence modules in a dataset. Previous learnable feature maps [HKNU17, CCI+20, RCB21] make the choice of *expressiveness* (being able to learn any arbitrary function on the space of persistence modules) over *stability* (learning a function under the constraint that it is robust to perturbations of the input). Moreover, since the methods are often parametrized by complex neural networks, it is difficult to compare and interpret parametrizations learned for different tasks. Our Wasserstein stable ranks are stable by construction. More precisely, the interleaving distance between Wasserstein stable ranks is 1-Lipschitz with respect to the corresponding Wasserstein distance used in its construction. Similarly to Wasserstein stable ranks, we also provide a simple formula for computing the interleaving distance between them at the cost of $O(n \log n)$ in the maximum number of bars in the two persistence modules we are comparing.

We use a metric learning framework to learn an optimal parametrization for a problem at hand, observe that a better model can be obtained by jointly optimizing the parameters p and the ones related to the contour C and illustrate that the output can be readily interpreted in terms of the learned parametrization focusing on e.g. global/local features or various parts of the filtration scale. The methods are demonstrated on a synthetic and a real-world datasets.

Outline of the paper. Section 2 contains background material. In Section 3 we prove results on the p -norm of the cokernel of a monomorphism and, dually, of the kernel of an epimorphism of persistence modules. Section 4 is a study of Wasserstein distances and their generalizations involving contours in the framework of noise systems. In Section 5 we compute Wasserstein stable ranks and interleaving distances between them, which we use to formulate a metric learning problem. In Section 6 we illustrate the use of Wasserstein stable ranks on synthetic and real-world data, learning optimal parameters of algebraic Wasserstein distances.

2 Preliminaries

2.1 Persistence modules and persistent homology

Let $[0, \infty)$ denote the totally ordered set of nonnegative real numbers, regarded as the category induced by the order structure. We consider an arbitrary fixed field K and denote by vect_K the category of finite dimensional vector spaces over K . A **persistence module over K** is a functor $X: [0, \infty) \rightarrow \text{vect}_K$. Explicitly, X consists of a collection of finite dimensional vector spaces X_t for all t in $[0, \infty)$, together with a collection of linear functions $X_{s \leq t}: X_s \rightarrow X_t$, called **transition functions**, for all $s \leq t$ in $[0, \infty)$, such that $X_{s \leq t} X_{r \leq s} = X_{r \leq t}$ for all $r \leq s \leq t$, and $X_{t \leq t}$ is the identity function on X_t for all t in $[0, \infty)$. A **morphism** or natural transformation $f: X \rightarrow Y$ between two persistence modules X and Y is a collection of linear functions $f_t: X_t \rightarrow Y_t$, for all t in $[0, \infty)$, such that $f_t X_{s \leq t} = Y_{s \leq t} f_s$ for all $s \leq t$ in $[0, \infty)$.

A persistence module X is **tame** if there exist real numbers $0 = t_0 < t_1 < \dots < t_k$ such that the transition function $X_{s \leq t}$ is a non-isomorphism only if $s < t_i \leq t$ for some $i \in \{1, \dots, k\}$. We denote by **Tame** the category of tame persistence modules and morphisms between them. The class of objects of this category will be denoted by **Tame** as well.

Convention 2.1. In this article we always work in the category of tame persistence modules

over a fixed field K . For brevity the term persistence module will be used to refer to tame persistence modules over K .

A morphism $f: X \rightarrow Y$ in \mathbf{Tame} is a monomorphism (respectively, an epimorphism or isomorphism) if the linear functions $f_t: X_t \rightarrow Y_t$ are monomorphisms (respectively, epimorphisms or isomorphisms) of vector spaces, for all t in $[0, \infty)$. Kernels, cokernels and direct sums in \mathbf{Tame} are defined componentwise. For example, for any persistence modules X and Y , the direct sum $X \oplus Y$ is the persistence module defined by $(X \oplus Y)_t = X_t \oplus Y_t$ and $(X \oplus Y)_{s \leq t} = X_{s \leq t} \oplus Y_{s \leq t}$, for all $s \leq t$ in $[0, \infty)$. The zero persistence module or **zero module**, i.e., the functor identically equal to the zero vector space on objects, will be denoted by 0 .

Let $a < b$ in $[0, \infty]$. We denote by $K(a, b)$ the persistence module defined as follows: for any t in $[0, \infty)$,

$$K(a, b)_t := \begin{cases} K & \text{if } a \leq t < b \\ 0 & \text{otherwise,} \end{cases}$$

and for any $s \leq t$ in $[0, \infty)$,

$$K(a, b)_{s \leq t} := \begin{cases} \text{id}_K & \text{if } K(a, b)_s = K = K(a, b)_t \\ 0 & \text{otherwise.} \end{cases}$$

We call $K(a, b)$ the **bar** (or interval module) with **start-point** a and **end-point** b . We say that the bar $K(a, b)$ is **infinite** if $b = \infty$ and **finite** otherwise. We say that the left-closed, right-open interval $[a, b)$ in $[0, \infty)$ is the **support** of the bar $K(a, b)$. As an easy consequence of naturality, a morphism $f: K(a_1, b_1) \rightarrow K(a_2, b_2)$ between bars can be nonzero (i.e. have some component f_a different from the zero map) only if $a_2 \leq a_1 < b_2 \leq b_1$. In this case, $\ker f$ is isomorphic to $K(b_2, b_1)$ if $b_2 < b_1$, and is zero otherwise, and $\text{coker } f$ is isomorphic to $K(a_2, a_1)$ if $a_2 < a_1$, and is zero otherwise.

A persistence module is **indecomposable** if, whenever it is isomorphic to a direct sum $Y \oplus Z$ with Y and Z in \mathbf{Tame} , either $Y = 0$ or $Z = 0$. Bars are indecomposable and, as the following fundamental result implies, any indecomposable in \mathbf{Tame} is isomorphic to a bar. We refer the reader to [CDSGO16] for more details on the algebraic structure of persistence modules.

Theorem 2.2 (Structure of persistence modules). *Any (tame) persistence module X is isomorphic to a finite direct sum of bars of the form $\bigoplus_{i=1}^k K(a_i, b_i)$, with $a_i < b_i$ in $[0, \infty]$ for every $i \in \{1, \dots, k\}$. This decomposition is unique up to permutation: if $X \cong \bigoplus_{i=1}^k K(a_i, b_i) \cong \bigoplus_{j=1}^{\ell} K(c_j, d_j)$, then $k = \ell$ and there exists a permutation σ on $\{1, \dots, k\}$ such that $a_i = c_{\sigma(i)}$ and $b_i = d_{\sigma(i)}$, for every $i \in \{1, \dots, k\}$.*

A decomposition of a persistence module X as a direct sum of bars as in Theorem 2.2 is called a **barcode decomposition** of X . In this article, we will occasionally denote a barcode decomposition of X by $\bigoplus_{i=1}^k X_i$ when we do not need an explicit notation for the bars' start- and end-points. The number k of bars in any barcode decomposition of X is called the **rank** of X , denoted by $\text{rank}(X)$.

Given a persistence module X , consider an element $x \in X_a$ for some a in $[0, \infty)$, and let $b := \sup\{t \in [a, \infty) \mid X_{a \leq t}(x) \neq 0\}$ in $[a, \infty]$. The element x is called a **generator** of X if the morphism $g: K(a, b) \rightarrow X$ defined by $g_a(1) = x$ is such that the composition rg with some

morphism $r: X \rightarrow K(a, b)$ is the identity on $K(a, b)$. We call $K(a, b)$ the **bar generated by x** , and we observe that it is a direct summand of X . We call a collection of elements $\{x_i \in X_{a_i}\}_{i=1}^k$ a **set of generators** of X if each x_i generates a bar $K(a_i, b_i)$ and the morphisms $g_i: K(a_i, b_i) \rightarrow X$ defined by x_i induce an isomorphism $\bigoplus_{i=1}^k K(a_i, b_i) \rightarrow X$.

As we will use basic homological algebra methods in **Tame**, we remark that infinite bars $K(a, \infty)$, for all a in $[0, \infty)$, are free in **Tame**, and that the notions of free and projective coincide in **Tame** (see [BM21] for details). Any bar $K(a, b)$ with $b < \infty$ admits a minimal free resolution of the form $0 \rightarrow K(b, \infty) \rightarrow K(a, \infty) \rightarrow K(a, b) \rightarrow 0$.

Remark 2.3. We note that $\text{rank}(X)$ can be viewed as a classical homological invariant corresponding to the number of generators in a minimal free resolution of X , which yields an alternative definition of the rank that is applicable to multiparameter persistence modules [SCL⁺17].

Lastly, let us briefly comment on a set theoretical detail regarding the category **Tame**. In **Tame**, the class of isomorphism classes of objects is a set, as a consequence of Theorem 2.2. In this article, we consider some class functions defined on **Tame**, referring to them simply as functions for brevity. Since all class functions on **Tame** we consider are constant on isomorphism classes of objects, they can be regarded as proper functions defined on the set of isomorphism classes of persistent modules.

2.2 Contours

Contours can be thought of as describing coherent ways to “flow” across the parameter space $[0, \infty)$ of persistence modules. In this article, we call **contour** a function $C: [0, \infty) \times [0, \infty) \rightarrow [0, \infty)$ such that, for all a, b, ε, τ in $[0, \infty)$, the following inequalities hold:

1. if $a \leq b$ and $\varepsilon \leq \tau$, then $C(a, \varepsilon) \leq C(b, \tau)$;
2. $a \leq C(a, 0)$;
3. $C(C(a, \varepsilon), \tau) \leq C(a, \varepsilon + \tau)$.

In [GC17] contours are defined in the case of n -parameter persistence modules. Contours are further studied for 1-parameter persistence in [CR20], where several concrete examples are given. In [CR20], the definition of contour is slightly more general than ours; for example, $C(a, \varepsilon)$ can take the value ∞ . Similar notions to contours appear in the literature by the name of *superlinear families of translations* [BDSS15] and *flows on posets* [dSMS18].

A contour C is called an **action** if the inequalities of (2.) and (3.) are equalities, that is, if $a = C(a, 0)$ and $C(C(a, \varepsilon), \tau) = C(a, \varepsilon + \tau)$, for all a, ε, τ . A contour C is **regular** [CR20] if the following conditions hold:

- $C(-, \varepsilon): [0, \infty) \rightarrow [0, \infty)$ is a monomorphism for all $\varepsilon \in [0, \infty)$;
- $C(a, -): [0, \infty) \rightarrow [0, \infty)$ is a monomorphism whose image is $[a, \infty)$, for all $a \in [0, \infty)$.

The second condition of regular contours ensures that $C(a, 0) = a$, for any a in $[0, \infty)$, and that C is strictly increasing in the second variable: $C(a, \varepsilon) < C(a, \tau)$ whenever $\varepsilon < \tau$, for any a in $[0, \infty)$.

Let C be a regular contour. For all $a \in [0, \infty)$, we define the function $\ell(a, -)$ to be the inverse of the function $C(a, -): [0, \infty) \rightarrow [a, \infty)$, that is, $\ell(a, b) = C^{-1}(a, -)(b)$ for any $b \in [a, \infty)$, and we set $\ell(a, \infty) = \infty$. We call ℓ the **lifetime function** associated with C . We observe that, since regular contours are injective functions in the second variable, $\ell(a, b)$ is well-defined for every pair $a \leq b$. Throughout the article, the **lifetime of a bar** $K(a, b)$ with respect to a contour C is the value $\ell(a, b)$ of the lifetime function associated with C .

As a first example of contour we consider the **standard contour**, a function D defined by $D(a, \varepsilon) = a + \varepsilon$, for every $a, \varepsilon \in [0, \infty)$. Informally, the standard contour describes the most uniform way to flow in the parameter space $[0, \infty)$ of a persistence module, linearly with unitary speed. We now introduce a large family of contours, called **integral contours of distance type** [CR20, ARSC21], parametrized by certain real-valued functions. Let $f: [0, \infty) \rightarrow (0, \infty)$ be a Lebesgue measurable function, called here a **density**. For every $a, \varepsilon \in [0, \infty)$, let $D_f(a, \varepsilon)$ be the real number in $[a, \infty)$ such that

$$\varepsilon = \int_a^{D_f(a, \varepsilon)} f(x) dx,$$

which is uniquely defined since f takes strictly positive values. The function $D_f: [0, \infty) \times [0, \infty) \rightarrow [0, \infty)$ is a contour; moreover, it is regular and an action. We observe that, if the density f is the constant function 1, the distance type contour D_1 coincides with the standard contour.

2.3 Noise systems

Noise systems provide a way to quantify the size of persistence modules and to produce pseudometrics on **Tame** by comparing their sizes [SCL⁺17]. A **noise system** on **Tame** is a sequence $\mathcal{S} = \{\mathcal{S}_\varepsilon\}_{\varepsilon \in [0, \infty)}$ of subclasses of **Tame** such that:

- $0 \in \mathcal{S}_\varepsilon$, for all ε ,
- $\mathcal{S}_\tau \subseteq \mathcal{S}_\varepsilon$ whenever $\tau \leq \varepsilon$,
- if $0 \rightarrow X_0 \rightarrow X_1 \rightarrow X_2 \rightarrow 0$ is a short exact sequence in **Tame**, then:
 - if $X_1 \in \mathcal{S}_\varepsilon$, then $X_0, X_2 \in \mathcal{S}_\varepsilon$,
 - if $X_0 \in \mathcal{S}_\varepsilon$ and $X_2 \in \mathcal{S}_\tau$, then $X_1 \in \mathcal{S}_{\varepsilon+\tau}$.

Given a noise system $\mathcal{S} = \{\mathcal{S}_\varepsilon\}_{\varepsilon \in [0, \infty)}$ it is natural to associate to each persistence module X the smallest ε such that $X \in \mathcal{S}_\varepsilon$. This defines a function $\alpha_{\mathcal{S}}: \mathbf{Tame} \rightarrow [0, \infty]$ called in [GNOW21] the **amplitude** associated to \mathcal{S} .

A noise system $\mathcal{S} = \{\mathcal{S}_\varepsilon\}_{\varepsilon \in [0, \infty)}$ is **closed under direct sums** if $X \oplus Y \in \mathcal{S}_\varepsilon$ whenever $X, Y \in \mathcal{S}_\varepsilon$, for every $\varepsilon \in [0, \infty)$. Contours (Section 2.2) provide examples of noise systems satisfying this property. Given a contour C and any $\varepsilon \in [0, \infty)$, let

$$\mathcal{S}_\varepsilon := \{X \in \mathbf{Tame} \mid X_{a \leq C(a, \varepsilon)} = 0 \text{ for all } a \in [0, \infty)\}.$$

It is proved in [GC17, Prop. 9.4] that the sequence $\{\mathcal{S}_\varepsilon\}_{\varepsilon \in [0, \infty)}$ defined in this way is a noise system closed under direct sums. In particular, the noise system induced by the standard contour

has components

$$\mathcal{S}_\varepsilon := \{X \in \mathbf{Tame} \mid X_{a \leq a+\varepsilon} = 0 \text{ for all } a \in [0, \infty)\},$$

and coincides with the **standard noise system** introduced in [SCL⁺17].

2.4 Pseudometrics between persistence modules

In this article, we call (extended) **pseudometric** on \mathbf{Tame} a function d assigning to any pair of persistence modules X, Y in \mathbf{Tame} an element $d(X, Y) \in [0, \infty]$ such that the following conditions hold for any X, Y, Z :

- $d(X, Y) = d(Y, X)$,
- $d(X, Y) = 0$ whenever X is isomorphic to Y ,
- $d(X, Z) \leq d(X, Y) + d(Y, Z)$.

The third condition, known as the triangle inequality, combined with the second one yields $d(X, Y) = d(X', Y')$ whenever $X \cong X'$ and $Y \cong Y'$. This definition of pseudometric coincides with Definition 3.3 in [BSS23] when considering the category \mathbf{Tame} .

We now briefly explain how noise systems yield pseudometrics on \mathbf{Tame} . Let \mathcal{S} be a noise system on \mathbf{Tame} . For any $\varepsilon \in [0, \infty)$, we say that two persistence modules X and Y are ε -**close** if there exists a persistence module Z and a pair of morphisms $X \xleftarrow{f} Z \xrightarrow{g} Y$ such that

$$\ker f \in \mathcal{S}_{\varepsilon_1}, \quad \text{coker } f \in \mathcal{S}_{\varepsilon_2}, \quad \ker g \in \mathcal{S}_{\varepsilon_3}, \quad \text{coker } g \in \mathcal{S}_{\varepsilon_4},$$

for some $\varepsilon_1, \varepsilon_2, \varepsilon_3, \varepsilon_4 \in [0, \infty)$ such that $\varepsilon_1 + \varepsilon_2 + \varepsilon_3 + \varepsilon_4 \leq \varepsilon$. Define

$$d_{\mathcal{S}}(X, Y) := \inf \{ \varepsilon \in [0, \infty) \mid X \text{ and } Y \text{ are } \varepsilon\text{-close} \},$$

adopting the convention $\inf \emptyset = \infty$. As shown in [SCL⁺17, Prop. 8.7], $d_{\mathcal{S}}$ is a pseudometric on \mathbf{Tame} .

We remark that the pseudometric $d_{\mathcal{S}}$ associated with the standard noise system is equivalent to the interleaving distance [Les15], as proved by [GC17, Prop. 12.2].

2.5 Hierarchical stabilization and stable rank

In the context of topological data analysis, **hierarchical stabilization** is a method to convert a discrete invariant of persistence modules into a stable invariant suitable for data analysis. This technique has been studied in [SCL⁺17, GC17] in the case of multiparameter persistence modules, and has been further investigated in [CR20] in the case of one-parameter persistence. Hierarchical stabilization has a very general formulation, which allows for several choices of discrete invariants, and in principle is not restricted to categories of persistence modules. For the hierarchical stabilization of the rank, also called stable rank, some computational methods have been developed [GC17, CR20]. In this article we will restrict our attention to the stable rank and further develop its computation.

Besides choosing a discrete invariant, hierarchical stabilization requires the choice of a pseudometric between persistence modules, which plays an active role in calculating the corresponding stable invariant. Consider the rank of a persistence module (Section 2.1) as a function $\text{rank}: \mathbf{Tame} \rightarrow \mathbb{N}$ mapping any persistence module X to the natural number $\text{rank}(X)$.

Definition 2.4. Given a pseudometric d on \mathbf{Tame} (Section 2.4), the **stable rank** of a persistence module X with respect to the pseudometric d is the function $\widehat{\text{rank}}_d(X): [0, \infty) \rightarrow [0, \infty)$ defined, for all $t \in [0, \infty)$, by

$$\widehat{\text{rank}}_d(X)(t) := \min\{\text{rank}(Y) \mid Y \in \mathbf{Tame} \text{ and } d(X, Y) \leq t\}.$$

We observe that the function $\widehat{\text{rank}}_d(X)$ is non-increasing and takes values in \mathbb{N} , so it belongs to the set \mathcal{M} of Lebesgue measurable functions $[0, \infty) \rightarrow [0, \infty)$.

To illustrate the stability of the invariant $\widehat{\text{rank}}_d$, we consider a pseudometric d_{\bowtie} on \mathcal{M} , called the **interleaving distance**, defined for all $f, g \in \mathcal{M}$ by

$$d_{\bowtie}(f, g) := \inf\{\varepsilon \in [0, \infty) \mid f(t) \geq g(t + \varepsilon) \text{ and } g(t) \geq f(t + \varepsilon), \text{ for all } t \in [0, \infty)\},$$

setting by convention $\inf \emptyset = \infty$. The stable rank then satisfies the following Lipschitz condition.

Proposition 2.5 ([SCL⁺17]). *Let d be a pseudometric on \mathbf{Tame} , and let X, Y be persistence modules. Then $d(X, Y) \geq d_{\bowtie}(\widehat{\text{rank}}_d(X), \widehat{\text{rank}}_d(Y))$.*

2.6 p -norms

In this subsection, we briefly review properties of p -norms that are useful for our work. For $p \in [1, \infty]$, the p -norm (also called L^p -norm) on \mathbb{R}^n is the function $\|\cdot\|_p: \mathbb{R}^n \rightarrow [0, \infty)$ defined, for each $x = (x_1, x_2, \dots, x_n) \in \mathbb{R}^n$, by

$$\|x\|_p := \begin{cases} (\sum_{i=1}^n |x_i|^p)^{\frac{1}{p}} & \text{for } p \in [1, \infty) \\ \max\{|x_i|\}_{i \in \{1, \dots, n\}} & \text{for } p = \infty. \end{cases}$$

We note that $\|x\|_\infty = \lim_{p \rightarrow \infty} \|x\|_p$, for all $x \in \mathbb{R}^n$. The triangle inequality (or subadditivity condition) $\|x + y\|_p \leq \|x\|_p + \|y\|_p$, for all $x, y \in \mathbb{R}^n$, is also referred to as Minkowski inequality.

A fundamental property of p -norms on \mathbb{R}^n is the following: for $x \in \mathbb{R}^n$ and for $1 \leq p \leq q \leq \infty$, the inequalities

$$\|x\|_q \leq \|x\|_p \leq n^{\left(\frac{1}{p} - \frac{1}{q}\right)} \|x\|_q \quad (2.1)$$

hold and are sharp, where by convention we set $\frac{1}{\infty} = 0$. We refer to the first inequality as the monotonicity property of p -norms.

The following elementary property of p -norms is useful in this work: for $p \in [1, \infty]$, if $x = (x_1, \dots, x_n) \in \mathbb{R}^n$, $y = (y_1, \dots, y_m) \in \mathbb{R}^m$ and $z = (x_1, \dots, x_n, y_1, \dots, y_m) \in \mathbb{R}^{n+m}$, then

$$\left\| \left(\|x\|_p, \|y\|_p \right) \right\|_p = \|z\|_p. \quad (2.2)$$

Finally, let us also observe that p -norms are permutation invariant, and that they preserve the order on $[0, \infty)^n$, meaning that if $x \leq y$ in $[0, \infty)^n$ according to the coordinate-wise order, then $\|x\|_p \leq \|y\|_p$.

In this article, we generally consider p -norms as functions from $[0, \infty)^n$ to $[0, \infty]$, extending the usual definition by setting $\|x\|_p = \infty$ whenever x has some coordinate $x_i = \infty$. All properties stated above still hold with this definition.

Following [ST20], we will consider p -norms of persistence modules, whose definition relies on the barcode decomposition (Section 2.1). For $p \in [1, \infty]$, the p -norm of a persistence module X having barcode decomposition $X \cong \bigoplus_{i=1}^k K(a_i, b_i)$ is defined by

$$\|X\|_p := \begin{cases} \left(\sum_{i=1}^k |b_i - a_i|^p \right)^{\frac{1}{p}} & \text{for } p \in [1, \infty) \\ \max\{|b_i - a_i|\}_{i \in \{1, \dots, k\}} & \text{for } p = \infty. \end{cases}$$

3 Monomorphisms, epimorphisms, and their p -norms

In this section we introduce bar-to-bar morphisms between persistence modules (Definition 3.1), which can informally be described as morphisms such that every bar in the barcode decomposition of the domain maps non-trivially to at most one bar in the barcode decomposition of the codomain. Our aim is proving results (Theorem 3.14 and Theorem 3.16) which compare monomorphisms and epimorphisms between two persistence modules to bar-to-bar monomorphisms and epimorphisms between the same persistence modules. These results allow one to reduce algebraic problems to much simpler combinatorial problems, as shown for example in Corollary 3.20 and Corollary 3.22.

3.1 Free presentations of monomorphisms

Given a monomorphism $f: Z \hookrightarrow X$ between persistence modules, we want to determine the barcode decomposition of $\text{coker } f$. We briefly describe a method that uses free resolutions of the persistence modules Z and X .

Consider the diagram

$$\begin{array}{ccccccccc} 0 & \longrightarrow & R_Z & \xrightarrow{i_Z} & G_Z & \xrightarrow{p_Z} & Z & \longrightarrow & 0 \\ & & \downarrow f_R & & \downarrow f_G & & \downarrow f & & \\ 0 & \longrightarrow & R_X & \xrightarrow{i_X} & G_X & \xrightarrow{p_X} & X & \longrightarrow & 0 \\ & & & & & & \downarrow q & & \\ & & & & & & \text{coker } f & & \end{array}$$

where the rows are (minimal) free resolutions of the persistence modules Z and X respectively, and q denotes the canonical epimorphism. The given morphism f induces a morphism $f_G: G_Z \rightarrow G_X$ between the modules of generators and a morphism $f_R: R_Z \rightarrow R_X$ between the modules of relations that make the diagram commutative (see e.g. [Rot09, Thm. 6.16]). We have $\text{coker } f \cong \text{coker}([f_G \ i_X]: G_Z \oplus R_X \rightarrow G_X)$, where the morphism $[f_G \ i_X]$ sends $(z, r) \in G_Z \oplus R_X$ to $f_G(z) + i_X(r)$. The isomorphism of cokernels is easy to prove, for example observing that the image of the composition qp_X is $\text{coker } f$ and verifying via diagram chasing that its kernel coincides with the image of $[f_G \ i_X]: G_Z \oplus R_X \rightarrow G_X$.

In other words, we have a free presentation of $\text{coker } f$

$$G_Z \oplus R_X \xrightarrow{[f_G \ i_X]} G_X \twoheadrightarrow \text{coker } f,$$

and we can use it to determine the barcode decomposition of $\text{coker } f$. More precisely, observing that $\text{coker } f$ is isomorphic to the homology at the middle term of the free chain complex

$$G_Z \oplus R_X \xrightarrow{[f_G \ i_X]} G_X \longrightarrow 0,$$

we can compute the barcode decomposition of $\text{coker } f$ by using the persistent homology algorithm on a matrix M_f representing the morphism $[f_G \ i_X]$, as we detail in Section 3.2. The persistent homology algorithm determines “pairings” of the basis elements of $G_Z \oplus R_X$ with the basis elements of G_X , which corresponds to the start- and end-point pairs of the bars of $\text{coker } f$.

In this section, we are interested in particular morphisms between persistence modules, which we call bar-to-bar morphisms.

Definition 3.1. A morphism $f: Z \rightarrow X$ of persistence modules is **bar-to-bar** if there are barcode decomposition $Z = \bigoplus_{i=1}^m Z_i$ and $X = \bigoplus_{j=1}^n X_j$ and there exist a subset $I \subseteq \{1, \dots, m\}$ and an injective function $\alpha: I \rightarrow \{1, \dots, n\}$ such that

$$f = \bigoplus_{i \in I} f_i \oplus \bigoplus_{i \in \{1, \dots, m\} \setminus I} g_i \oplus \bigoplus_{j \in \{1, \dots, n\} \setminus \alpha(I)} h_j, \quad (3.1)$$

where each $f_i := f|_{Z_i}$ is a nonzero morphism $Z_i \rightarrow X_{\alpha(i)}$, and where g_i denotes the zero morphism $Z_i \rightarrow 0$ and h_j denotes the zero morphism $0 \rightarrow X_j$.

Remark 3.2. If f is a bar-to-bar morphism as in (3.1), then $\ker f$ and $\text{coker } f$ are easily determined recalling the case of a morphism between two bars (see Section 2.1), namely:

$$\ker f = \bigoplus_{i \in I} \ker f_i \oplus \bigoplus_{i \in \{1, \dots, m\} \setminus I} Z_i, \quad \text{coker } f = \bigoplus_{i \in I} \text{coker } f_i \oplus \bigoplus_{j \in \{1, \dots, n\} \setminus \alpha(I)} X_j.$$

Furthermore, if f is a monomorphism, the fact that $\ker f$ vanishes implies that $I = \{1, \dots, m\}$, and the existence of the injective function α implies $m \leq n$. Dually, $\alpha(I) = \{1, \dots, n\}$ and $n \leq m$ if f is an epimorphism.

The main result of this section is the following (Theorem 3.14): given any monomorphism $f: Z \hookrightarrow X$, there is a bar-to-bar monomorphism $f_b: Z \hookrightarrow X$ such that $\|\text{coker } f_b\|_p \leq \|\text{coker } f\|_p$ for any $p \in [1, \infty]$. A dual statement (Theorem 3.16) holds for kernels of epimorphisms.

3.2 Finding monomorphisms with smaller cokernels

To prove our inequalities between p -norms of cokernels, we modify a strategy used in [ST20, Sect. 7.1] to obtain new inequalities between p -norms of persistence modules, based on the rearrangement inequality (Theorem 3.12) and on the comparison of pairings in certain barcode decompositions using the persistent homology algorithm. For simplicity, we fix the field with two elements \mathbb{F}_2 as the base field in this subsection, but our results work for any base field.

Let Z and X be persistence modules and $f: Z \hookrightarrow X$ a monomorphism of persistence modules. Fix $\{z_i\}_{i=1}^m$ and $\{x_j\}_{j=1}^n$ sets of generators of Z and X , respectively, and denote by $Z = \bigoplus_{i=1}^m K(a_i^z, b_i^z)$ and $X = \bigoplus_{j=1}^n K(a_j^x, b_j^x)$ the respective barcode decompositions. That is, for every z_i , a_i^z is the **degree** of $z_i \in Z_{a_i^z}$ and b_i^z is the end-point of the bar generated by z_i , and similarly for the x_j . In this section, we assume for the ease of exposition that X has no infinite bars in its decomposition. All the results we present can be adapted to the general case by setting $b_j^x = \infty$ whenever x_j generates an infinite bar. Throughout this section, we will consider

on matrix reduction via left-to-right column operation, like the so-called standard algorithm for persistent homology [ELZ00, ZC05] (see Algorithm 1 in [OPT⁺17] for a description). Even though these methods are usually presented for filtered simplicial complexes in the literature, they extend to graded free chain complexes as in our case. The barcode decomposition (of coker f in our case) can be read out from a reduced matrix, and does not depend on the way of reducing the matrix via left-to-right column operations (see Lemma 3.5).

Let \bar{M}_f be a complete reduction of M_f by left-to-right column transformations, where a matrix is said to be **reduced** if no two columns have their lowest nonzero entry on the same row. Let σ_f be the function that to the k^{th} nonzero column of \bar{M}_f associates the row of its lowest nonzero entry, for every $k \in \{1, \dots, n\}$. We know that σ_f is a permutation on $\{1, \dots, n\}$ since the n columns of M_f in C_X are linearly independent. In this section, we use square brackets for a permutation $\sigma = [\sigma(1) \cdots \sigma(n)]$ on $\{1, \dots, n\}$ expressed in one-line notation, to distinguish it from the notation for cycles, denoted by $(c_1 c_2 \cdots c_\ell)$. For the running example (3.3), we get

$$\bar{M}_f = \left[\begin{array}{c|c|c|c|c|c|c} \boxed{0} & & & & & & \\ \boxed{0} & & & & & & \\ \boxed{0} & & & & & & \\ \boxed{1} & \boxed{1} & & & & & \\ \boxed{1} & 0 & & & & & \\ \boxed{0} & & & & & & \\ \hline & & \boxed{0} & \boxed{1} & & & \\ & & \boxed{0} & \boxed{1} & & & \\ & & \boxed{1} & \boxed{0} & & & \\ & & \boxed{0} & \boxed{0} & & & \\ & & \boxed{0} & \boxed{0} & & & \\ & & \boxed{0} & \boxed{1} & & & \\ \hline & & & & 0 & & \\ & & & & 0 & & \\ & & & & & \boxed{1} & \\ & & & & & & \boxed{1} \\ & & & & & & 0 \\ & & & & & & 0 \end{array} \right],$$

where we have outlined the lowest nonzero coefficient of each column, and so $\sigma_f = [543621]$. We do not need to specify the order of transformations in this reduction thanks to the following lemma, which is a consequence of the pairing uniqueness lemma of [CSEM06, Sect. 3].

Lemma 3.5. *The permutation σ_f is well-defined. In particular, it does not depend on the choice of a sequence of left-to-right column operations to obtain a reduced matrix from M_f .*

By design of the persistent homology algorithm, a barcode decomposition of coker f is completely determined by σ_f together with the degrees of the generators of Z and X . In Corollary 3.11 we will provide a precise statement.

From the matrix M_f we define the **bar-to-bar matrix** M_b by Algorithm 1. The bar-to-bar matrix M_b is the presentation matrix of a **bar-to-bar monomorphism** $f_b: Z \hookrightarrow X$ having the same domain and codomain as f .

Algorithm 1 also partially reduces M_f and constructs an injective function $r_{\max}: C_Z \rightarrow C_X$. Given a column z in C_Z , we call $r_{\max}(z)$ its **rightmost matched column**. Informally, Algorithm 1 computes the bar-to-bar matrix M_b by setting to zero each column z of M_f in C_Z except for the nonzero entry on the unique row x such that $M_f(x, r_{\max}(z)) = 1$. For example, starting with the matrix M_f from (3.3), we get

$$\left[\begin{array}{c|c|c|c|c|c|c} \boxed{0} & & & & & & \\ \boxed{0} & & & & & & \\ \boxed{0} & & & & & & \\ \boxed{1} & \boxed{1} & & & & & \\ \boxed{1} & 1 & & & & & \\ \boxed{0} & & & & & & \\ \hline & & \boxed{0} & \boxed{1} & & & \\ & & \boxed{0} & \boxed{1} & & & \\ & & \boxed{1} & \boxed{0} & & & \\ & & \boxed{0} & \boxed{0} & & & \\ & & \boxed{0} & \boxed{1} & & & \\ \hline & & & & & & 1 \\ & & & & & & \boxed{1} \\ & & & & & & \boxed{1} \\ & & & & & & 1 \end{array} \right],$$

that the end-point of the bar of X generated by x has degree strictly larger than the degree of z . Lastly, the cardinality of $\Gamma(z)$ equals the number of nonzero entries of z because the columns in C_X form a permutation matrix of rank n . \square

Proposition 3.7. *Let $f: Z \hookrightarrow X$ be a monomorphism and let M_f be a presentation matrix of f . The execution of Algorithm 1 on M_f returns a well-defined function $r_{\max}: C_Z \rightarrow C_X$ that is injective. Furthermore, for every column $z \in C_Z$, the column $r_{\max}(z)$ is to the right of z .*

Proof. We prove that, for every column $z \in C_Z$, $r_{\max}(z)$ is well-defined and to the right of z . We proceed by induction on $m := |C_Z|$, proving the result for all monomorphisms $f: Z \hookrightarrow X$ with presentations such that $|C_Z| = m$.

If $m = 1$ and $C_Z = \{z\}$, then the algorithm sets $r_{\max}(z)$ to be the rightmost column in C_X having a nonzero entry on the same row as a nonzero entry of z , which exists and is to the right of z by Proposition 3.6.

Now suppose that the statement holds for every monomorphism presentation matrix with m columns in C_Z . Let M_f be a presentation matrix such that $|C_Z| = m + 1$. Algorithm 1 performs a ‘for’ loop (line 4) until the ‘if’ statement (line 6) is true, which by Proposition 3.6 must happen before the algorithm terminates. Let r_0 be the rightmost column in C_X such that there is a (minimal, i.e. leftmost) $z \in C_Z$ with $M_f(x, z) = 1$, where x is the row associated to r_0 . Again by Proposition 3.6, column r_0 is to the right of column z . The reductions in lines 11-14 of the algorithm transform M_f into a matrix M_f^* presenting a different monomorphism $f': Z \hookrightarrow X$. The morphism f' coincides with f on all generators of Z except for generator z' , which is mapped to the nonzero element $f_{a^{z'}}(z') + f_{a^z}(Z_{a^z \leq a^{z'}}(z))$, where a^z and $a^{z'}$ respectively denote the degrees of z and z' . We see that f' is a monomorphism via the following pointwise argument. For every degree a , the linear function $f_a: Z_a \rightarrow X_a$ has $\ker f_a = 0$, hence it maps nonzero elements in $\{Z_{a^z \leq a}(z_i)\}_{i=1}^m$ to linearly independent elements $\{y_j\}$ in $\text{span}(X_{a^z \leq a}(x_j))_{j=1}^n$. We see that $f'_a: Z_a \rightarrow X_a$ satisfies the same linear independence property (which implies $\ker f'_a = 0$) because the set of image elements coincides, except for possibly an element y' replaced by $y' + y$, where y is a different element of the set.

In M_f^* , the only column in C_Z with nonzero entry in row x is z . By removing column z and row x , we obtain a matrix with m columns in C_Z which is again a presentation matrix of a monomorphism. By induction hypothesis we know that the algorithm determines a function $r'_{\max}: C_Z \setminus \{z\} \rightarrow C_X$ whose image does not contain r_0 and the columns to its right. The function r'_{\max} extends to a function $r_{\max}: C_Z \rightarrow C_X$ by defining $r_{\max}(z) := r_0$. Finally, we observe that the function r_{\max} is injective by construction. \square

Let us now go back to the reduction of presentation matrices. As with M_f , we can reduce M_b by left-to-right column transformations to get a reduced matrix \bar{M}_b . We denote by σ_b the permutation on $\{1, \dots, n\}$ associated with the nonzero columns of \bar{M}_b , which is well-defined because the matrix M_b only has columns with at most one nonzero coefficient and has the same set of columns in C_X as M_f . In our running example, computing \bar{M}_b gives us $\sigma_b = [453261]$.

After reduction via left-to-right column operations, the matrices \bar{M}_f and \bar{M}_b have non-zero columns with the same set of labels, as we will prove in Proposition 3.9.

Definition 3.8. Let $n \geq 1$ be an integer and σ a permutation on $\{1, \dots, n\}$. An **inversion** of σ is a pair (i, j) of elements of $\{1, \dots, n\}$ such that $i < j$ and $\sigma(i) > \sigma(j)$.

Given a permutation σ , we also give the name **inversion** to a transposition $(i j)$ such that $i < j$ and $\sigma(i) < \sigma(j)$: composing σ by $(i j)$ on the right creates an inversion.

Using inversions we can define a poset structure on permutations: we write $\sigma \leq \sigma'$ if there exist $k \geq 0$ and a composition of transpositions $\tau = \tau_1 \cdots \tau_k$ such that $\sigma\tau = \sigma'$ and, for all $i \leq k$, τ_i is an inversion of the permutation $\sigma\tau_1 \cdots \tau_{i-1}$. In what follows, we often call τ simply a **composition of inversions of σ** when it satisfies this property. Notice that \leq is a partial order on S_n , the symmetric group on $\{1, \dots, n\}$. With respect to this order, the identity permutation is the smallest element and the reverse permutation $[n \ n-1 \ \dots \ 2 \ 1]$ is the largest element.

Proposition 3.9. *Let $f: Z \hookrightarrow X$ be a monomorphism, M_f be a presentation matrix of f and M_b be the bar-to-bar matrix computed via Algorithm 1. Let \bar{M}_f and \bar{M}_b be reduced matrices obtained from M_f and M_b respectively, and let σ_f and σ_b be the associated permutations. Then, the following facts hold:*

- *the nonzero columns of the reduced matrices \bar{M}_f and \bar{M}_b are in the same positions,*
- *$\sigma_f \geq \sigma_b$, that is, $\sigma_f = \sigma_b\tau$ with τ a composition of inversions of σ_b .*

Proof. Since we can replace M_f with the output M_f^* of Algorithm 1, which has the same associated permutation σ_f (as it is obtained by partially reducing M_f), we can assume that M_f satisfies the following property: for every column z in C_Z , the only row x such that $M_f(x, r_{\max}(z)) = 1$ has exactly one other nonzero entry, which is $M_f(x, z) = 1$. We prove the claims by induction on the number of columns in C_Z .

If $C_Z = \emptyset$, then there is nothing to prove: $M_f = M_b$ and they are reduced, so $\sigma_f = \sigma_b$.

Otherwise, we execute Algorithm 1 to get the bar-to-bar matrix M_b and the function r_{\max} . Let z_0 be the unique column of M_f in C_Z such that $r_0 := r_{\max}(z_0)$ is maximal in the total order on columns. By removing column z_0 , we obtain a presentation matrix M'_f of a monomorphism f' with a set of columns C'_Z strictly contained in C_Z , to which we can apply our induction hypothesis: \bar{M}'_f and \bar{M}'_b have the same nonzero columns, and $\sigma'_f = \sigma'_b\tau$ for some composition of inversions τ of σ'_b . The matrix M'_b , computed by using Algorithm 1 on M'_f , can be equivalently obtained by removing column z_0 from M_b , since M_f satisfies the property stated at the beginning of the proof. See Example 3.10 for matrices M'_f , M'_b , \bar{M}'_f and \bar{M}'_b in the running example.

Let x_0 be the only row such that $M_f(x_0, r_0) = 1$. By the execution of Algorithm 1, no other column of M'_f has a nonzero coefficient on row x_0 , and so we deduce that the reductions of the matrices M'_f and M'_b do not affect column r_0 . Since by inductive hypothesis M'_f and M'_b have the same nonzero columns, this implies that column r_0 does not appear in the inversions of τ , meaning that $\tau = (s_1 t_1)(s_2 t_2) \cdots (s_k t_k)$ with $s_i \neq c'_{r_0}$ and $t_i \neq c'_{r_0}$ for all $i \in \{1, \dots, k\}$, where c'_{r_0} denotes the relative position in $\{1, \dots, n\}$ of column r_0 in the (totally ordered) set of nonzero columns of the reduced matrix \bar{M}'_b .

Now, let M_g be the matrix M_f where we modify the column z_0 by setting to zero all its entries except the one on row x_0 . We reduce the matrix M_f first as for M'_f , and then we reduce the column z_0 by columns to its left, which does not affect the nonzero coefficient on row x_0 : we denote the resulting matrix by M''_f . \bar{M}_f is then obtained by completing the reduction using

column z_0 . We reduce M_g and M_b in similar fashion, following M'_f and M'_b , respectively. We observe the following facts.

- The nonzero columns of \bar{M}_f , \bar{M}_g , and \bar{M}_b are the nonzero columns of \bar{M}'_f and \bar{M}'_b , except we replace r_0 with z_0 . This is clear by construction for the matrices \bar{M}_g and \bar{M}_b , as the column z_0 coincides with r_0 . For the matrix \bar{M}_f , observe that for every nonzero entry $M_f(x, z_0)$ on column z_0 , there is a nonzero entry $M_f(x, r)$ in a column r to the left of r_0 , which implies that r_0 gets zeroed out after the reduction as it is linearly dependent with a number of columns to its left.
- $\sigma_f = \sigma_g \tau'$ where $\tau' := (c_{z_0} c_1)(c_1 c_2) \cdots (c_{k-1} c_k)$ and c_1, \dots, c_k, c_{r_0} are the relative positions in $\{1, \dots, n\}$ of the nonzero columns of M'_f whose lowest nonzero entry is modified (is moved to a different row) when reducing to \bar{M}_f , with c_{z_0} and c_{r_0} respectively denoting the relative positions of column z_0 and r_0 in the set of nonzero columns of M'_f .
- $\sigma_g = \sigma'_f \gamma^{-1}$ and $\sigma_b = \sigma'_b \gamma^{-1}$ where $\gamma := (c_{z_0} c_{z_0+1} \cdots c_{r_0})$ represents a cyclic permutation of the nonzero columns between z_0 and r_0 .

See Example 3.10 for concrete examples of these relationships. We deduce that

$$\begin{aligned} \sigma_f &= \sigma_g \tau' \\ &= \sigma'_f \gamma^{-1} \tau' \\ &= \sigma'_b \tau \gamma^{-1} \tau' \\ &= \sigma_b \gamma \tau \gamma^{-1} \tau'. \end{aligned}$$

By the definition of τ' , it is a composition of inversions of σ_g . We conclude the induction step by showing that $\gamma \tau \gamma^{-1}$ is a composition of inversions of σ_b .

More precisely, we know that $\tau = (s_1 t_1) \cdots (s_k t_k)$ is a composition of inversions of σ'_b , meaning that $(s_i t_i)$ is an inversion of the permutation $\sigma'_b(s_1 t_1) \cdots (s_{i-1} t_{i-1})$, for every $i \in \{1, \dots, k\}$, and we want to prove that $\gamma \tau \gamma^{-1} = (\gamma(s_1) \gamma(t_1)) \cdots (\gamma(s_k) \gamma(t_k))$ is a composition of inversions of σ_b , meaning that $(\gamma(s_i) \gamma(t_i))$ is an inversion of the permutation $\sigma_b(\gamma(s_1) \gamma(t_1)) \cdots (\gamma(s_{i-1}) \gamma(t_{i-1}))$, for every $i \in \{1, \dots, k\}$. First, we observe that $s_i < t_i$ implies $\gamma(s_i) < \gamma(t_i)$, since as observed earlier the relative position c'_{r_0} of column r_0 in the set of nonzero columns of \bar{M}'_b does not appear in τ . Let us now denote

$$\begin{aligned} \sigma'_{i-1} &:= \sigma'_b(s_1 t_1) \cdots (s_{i-1} t_{i-1}), \\ \sigma_{i-1} &:= \sigma_b(\gamma(s_1) \gamma(t_1)) \cdots (\gamma(s_{i-1}) \gamma(t_{i-1})). \end{aligned}$$

We have to prove that $\sigma'_{i-1}(s_i) < \sigma'_{i-1}(t_i)$ implies $\sigma_{i-1}(\gamma(s_i)) < \sigma_{i-1}(\gamma(t_i))$. This is a consequence of the equalities

$$\sigma_{i-1}(\gamma(s_i)) = \sigma_b \gamma(s_1 t_1) \gamma^{-1} \gamma \cdots \gamma^{-1} \gamma(s_{i-1} t_{i-1}) \gamma^{-1} \gamma(s_i) = \sigma'_{i-1}(s_i)$$

and of similar equalities for t_i . □

Theorem 3.12 (Rearrangement inequality). *Let g_1, g_2, \dots, g_n be real valued functions defined on an interval $I \subseteq \mathbb{R}$ such that $g_{k+1} - g_k$ is a non-decreasing function, for all $k \in \{1, \dots, n-1\}$, and let $b_1 \leq b_2 \leq \dots \leq b_n$ be a sequence of elements of I . If $\rho \leq \sigma$ in S_n , then*

$$\sum_{k=1}^n g_k(b_{\rho(k)}) \geq \sum_{k=1}^n g_k(b_{\sigma(k)}).$$

Proof. Since the argument we present can be iterated, it is enough to prove the statement for $\sigma = \rho\tau$ where $\tau = (i j)$ is an inversion: $i < j$ and $\rho(i) < \rho(j)$. We have

$$\begin{aligned} \sum_{k=1}^n g_k(b_{\rho(k)}) - \sum_{k=1}^n g_k(b_{\sigma(k)}) &= g_i(b_{\rho(i)}) + g_j(b_{\rho(j)}) - g_i(b_{\sigma(i)}) - g_j(b_{\sigma(j)}) \\ &= g_i(b_{\rho(i)}) + g_j(b_{\rho(j)}) - g_i(b_{\rho(j)}) - g_j(b_{\rho(i)}) \\ &= \left(g_j(b_{\rho(j)}) - g_i(b_{\rho(j)}) \right) - \left(g_j(b_{\rho(i)}) - g_i(b_{\rho(i)}) \right) \geq 0, \end{aligned}$$

where the last inequality follows from $b_{\rho(i)} \leq b_{\rho(j)}$ and from the fact that $g_j - g_i$ is non-decreasing. \square

Corollary 3.13. *Let $a_1 \leq a_2 \leq \dots \leq a_n$ and $b_1 \leq b_2 \leq \dots \leq b_n$ be sequences of real numbers, and let $p \in [1, \infty)$. If $\rho \leq \sigma$ in S_n , then*

$$\sum_{k=1}^n |a_k - b_{\rho(k)}|^p \leq \sum_{k=1}^n |a_k - b_{\sigma(k)}|^p.$$

Proof. Let $h_k(x) = |a_k - x|^p$. It is easy to check that the function $h_{k+1} - h_k$ is non-increasing for all $k \in \{1, \dots, n-1\}$, so we can apply Theorem 3.12 to the sequence of functions $g_k := -h_k$. \square

Theorem 3.14. *For any monomorphism $f: Z \hookrightarrow X$ it is possible to determine (via Algorithm 1) a bar-to-bar monomorphism $f_b: Z \hookrightarrow X$ such that $\|\text{coker } f_b\|_p \leq \|\text{coker } f\|_p$, for all $p \in [1, \infty)$.*

Proof. First, assume $p \in [1, \infty)$. The persistence modules $\text{coker } f$ and $\text{coker } f_b$ have barcode decompositions as in Corollary 3.11. Then, the claim follows from Corollary 3.13 applied to the permutations $\sigma_b \leq \sigma_f$ (Proposition 3.9). The claim for $p = \infty$ follows from taking the limit for $p \rightarrow \infty$ of both sides of the inequality $\|\text{coker } b\|_p \leq \|\text{coker } f\|_p$, recalling that $\lim_{p \rightarrow \infty} \|u\|_p = \|u\|_\infty$ for any vector $u \in \mathbb{R}^n$ (Section 2.6). \square

3.3 Bar-to-bar epimorphisms

A similar result to Theorem 3.14 exists for epimorphisms and their kernels. To show this, we use a duality argument. The dualization of persistence modules has been studied extensively, see e.g. [BL15, Mil20, BS23]. Here we dualize tame persistence modules indexed by $[0, \infty)$, which requires some special handling since in our setting bars are only supported on left-closed right-open intervals. To simplify the exposition, we explicitly work with finite direct sums of bars instead of general tame persistence modules, which are only equal to direct sums of bars up to isomorphism.

Definition 3.15. Let $\text{Bar}_{[0, \infty)}$ be the full subcategory of tame persistence modules whose objects are finite direct sums of bars. Similarly, let $\text{Bar}_{(-\infty, 0]}$ be the category of finite direct sums of bars indexed by the poset $(-\infty, 0]$ with the usual order. These categories are abelian and we can represent morphisms as matrices of morphisms between summands.

We consider the contravariant functor $(-)^{\vee}: \mathbf{Bar}_{[0,\infty)} \rightarrow \mathbf{Bar}_{(-\infty,0]}$ sending an object X in $\mathbf{Bar}_{[0,\infty)}$ to the functor $X^{\vee}: (-\infty,0] \rightarrow \mathbf{vect}_K$ defined, for all $s \leq t$ in $(-\infty,0]$, by $X_t^{\vee} := \mathbf{hom}(X_{-t}, K)$ and $X_{s \leq t}^{\vee} := \mathbf{hom}(X_{-t \leq -s}, K)$. Similarly, a contravariant functor $\mathbf{Bar}_{[0,\infty)} \rightarrow \mathbf{Bar}_{(-\infty,0]}$ is defined, which we also denote by $(-)^{\vee}$ with an abuse of notation. Both functors $(-)^{\vee}$ are exact.

If $X = K(a, b)$, we observe that X^{\vee} is also a bar, but its support (i.e., the set of poset elements for which the functor X^{\vee} takes a nonzero value) is the left-open, right-closed interval $(-b, -a]$. In this article, we are considering bars whose support is a left-closed, right-open interval in \mathbb{R} . To fix this, we can consider the **pointwise direct limit** functor $\varinjlim_{[0,-)}(-): \mathbf{Bar}_{[0,\infty)} \rightarrow \mathbf{Bar}_{[0,\infty)}$ sending X to the persistence module whose value at t is $\varinjlim_{t < a} X_t$ and whose transition functions are naturally defined. If $X = K(a, b)$, applying the pointwise direct limit functor yields the bar supported on $(a, b]$, whose dual $K(a, b)^{\vee}$ is the bar $K(-b, -a)$ in $\mathbf{Bar}_{(-\infty,0]}$, which is supported on $[-b, -a)$. Similarly, one defines the pointwise direct limit functor $\varinjlim_{(-\infty,-)}(-): \mathbf{Bar}_{(-\infty,0]} \rightarrow \mathbf{Bar}_{(-\infty,0]}$. The pointwise direct limit functors are exact. Applying the functor $(-)^{\vee}$ after the pointwise direct limit functor is therefore an exact functor, which we denote by $(-)^{\dagger}$.

To summarize, we have contravariant exact functors

$$(-)^{\dagger}: \mathbf{Bar}_{[0,\infty)} \rightarrow \mathbf{Bar}_{(-\infty,0]} \quad \text{and} \quad (-)^{\dagger}: \mathbf{Bar}_{(-\infty,0]} \rightarrow \mathbf{Bar}_{[0,\infty)}$$

sending a bar $K(a, b)$ supported on $[a, b)$ to the bar $K(-b, -a)$ supported on $[-b, -a)$, and extended to the rest of the objects by additivity. These functors send morphisms to their transpose (when viewed as matrices). More precisely, given a morphism $f: \bigoplus_i K(a_i, b_i) \rightarrow \bigoplus_j K(c_j, d_j)$ written as the matrix $[f_{i,j}]_{i,j}$ with $f_{i,j}: K(a_i, b_i) \rightarrow K(c_j, d_j)$ for all i and j , the morphism $f^{\dagger}: \bigoplus_j K(-d_j, -c_j) \rightarrow \bigoplus_i K(-b_i, -a_i)$ can be written as the matrix $[f_{j,i}^{\dagger}]_{i,j}$.

As a consequence of the exactness of $(-)^{\dagger}$, for any morphism $f: X \rightarrow Y$ in $\mathbf{Bar}_{[0,\infty)}$ (resp. in $\mathbf{Bar}_{(-\infty,0]}$) we have

$$(\ker f)^{\dagger} \cong \mathbf{coker} f^{\dagger} \quad \text{and} \quad (\mathbf{coker} f)^{\dagger} \cong \ker f^{\dagger}.$$

Since the functors $(-)^{\dagger}$ send morphisms to their transpose, they send bar-to-bar morphisms to bar-to-bar morphisms. In particular, they send bar-to-bar monomorphisms to bar-to-bar epimorphisms, and vice-versa. It is also clear that the functors $(-)^{\dagger}$ preserve p -norms: $\|X^{\dagger}\|_p = \|X\|_p$.

Moreover, we can apply the theory of Section 3.2 to the category $\mathbf{Bar}_{(-\infty,0]}$, and in particular apply Theorem 3.14. We conclude with the following result:

Theorem 3.16. *For any epimorphism $f: Z \twoheadrightarrow X$ of persistence modules, it is possible to determine a bar-to-bar epimorphism $f_b: Z \twoheadrightarrow X$ such that $\|\ker f_b\|_p \leq \|\ker f\|_p$, for all $p \in [1, \infty]$.*

Proof. As for the case of monomorphisms, we assume that X and Z are finite direct sums of finite bars. We apply Theorem 3.14 to $f^{\dagger}: X^{\dagger} \hookrightarrow Z^{\dagger}$ to get a bar-to-bar monomorphism g . We set $f_b := g^{\dagger}: Z \twoheadrightarrow X$ a bar-to-bar epimorphism, and we observe that

$$\|\ker f_b\| = \|\mathbf{coker} g\| \leq \|\mathbf{coker} f^{\dagger}\| = \|\ker f\|.$$

□

3.4 Comparing bar-to-bar morphisms with induced matchings

In [BL15] the authors introduce a construction similar to bar-to-bar morphisms, namely **induced matchings**. In particular, given persistence modules X and Z such that there exists a monomorphism $Z \hookrightarrow X$, the authors define a **canonical injection** from the multiset of bars of Z to the multiset of bars of X , where for all real numbers $b \in [0, \infty]$ the i^{th} longest bar of Z with end-point b is sent to the i^{th} longest bar of X with the same end-point. This injection induces a bar-to-bar monomorphism, which we define here:

Definition 3.17. Let Z and X be persistence modules such that there exists a monomorphism $Z \hookrightarrow X$, and fix barcode decompositions $Z = \bigoplus_{i=1}^m K(a_i^z, b_i^z)$ and $X = \bigoplus_{j=1}^n K(a_j^x, b_j^x)$. The induced matching of [BL15] then corresponds to a canonical injection $\varphi: \{1, \dots, m\} \hookrightarrow \{1, \dots, n\}$.

We define the **monomorphism induced by the canonical injection** φ as the monomorphism $f_\varphi: Z \hookrightarrow X$ given by

$$f_\varphi = \bigoplus_{i=1}^m (K(a_i^z, b_i^z) \hookrightarrow K(a_{\varphi(i)}^x, b_{\varphi(i)}^x)) \oplus \bigoplus_{j \in \{1, \dots, n\} \setminus \text{im } \varphi} (0 \hookrightarrow K(a_j^x, b_j^x)).$$

Note that this is a bar-to-bar monomorphism.

Remark 3.18. Let $f: Z \hookrightarrow X$ be a monomorphism. If the bars of X all have distinct end-points, then the monomorphism induced by the canonical injection (Definition 3.17) coincides, up to isomorphism, with the bar-to-bar monomorphism f_b as determined in Section 3.2. This is because, in this case, there is only one bar-to-bar monomorphism from Z to X (up to isomorphism).

Remark 3.19. In general, this is not necessarily the case. For example, starting from the monomorphism $f: K(2, 3) \hookrightarrow K(1, 3) \oplus K(2, 3)$ defined by

$$f = (K(2, 3) \hookrightarrow K(2, 3)) \oplus (0 \hookrightarrow K(1, 3)),$$

then we have $f_\varphi = (K(2, 3) \hookrightarrow K(1, 3)) \oplus (0 \hookrightarrow K(2, 3))$, while $f_b = f$.

More generally, monomorphisms induced by canonical injections do not commute with direct sums of monomorphisms [BL15, Example 5.8], while the bar-to-bar monomorphisms we introduced in Section 3.2 do, as an immediate consequence of their definition via Algorithm 1. That is, given $f: Z \hookrightarrow X$ and $f': Z' \hookrightarrow X'$, it is not true in general that $(f \oplus f')_\varphi = f_\varphi \oplus f'_\varphi$, while $(f \oplus f')_b = f_b \oplus f'_b$ holds.

Maintaining a close relation between a given monomorphism $f: Z \hookrightarrow X$ and the bar-to-bar monomorphism f_b was instrumental to prove Proposition 3.9, the key technical result of Section 3.2, and in turn Theorem 3.14 and the dual Theorem 3.16. Since the canonical injection [BL15] does not depend on the specific given monomorphism between Z and X , but just on the existence of such a monomorphism, it is not possible to prove Proposition 3.9 using the same strategy with the canonical injection instead of the bar-to-bar monomorphism we introduced.

We conclude this section with two corollaries to Theorem 3.14 and Theorem 3.16. Using Theorem 3.14, the problem of minimizing the p -norm of cokernels of all possible monomorphisms between two given persistence modules can be solved by restricting to bar-to-bar monomorphisms. This simplification allows for an easy combinatorial proof of the fact that, among all bar-to-bar monomorphisms, the one induced by the canonical injection minimizes the p -norm of the cokernel. A dual result holds for epimorphisms.

Corollary 3.20. *Let Z and X be two persistence modules such that there exists a monomorphism $Z \hookrightarrow X$. Then $\min_f: Z \hookrightarrow X \|\operatorname{coker} f\|_p = \|\operatorname{coker} f_\varphi\|_p$ for all $p \in [1, \infty]$, where f_φ is the bar-to-bar monomorphism induced by the canonical injection (Definition 3.17).*

Proof. By Theorem 3.14, it suffices to show the inequality $\|\operatorname{coker} f_\varphi\|_p \leq \|\operatorname{coker} f\|_p$ for bar-to-bar monomorphisms $f: Z \hookrightarrow X$. Let $\{b_k\}_{k=1}^\ell$ be the set of distinct end-points of X . Then, by hypothesis that there exists a monomorphism $Z \hookrightarrow X$, we can decompose $Z = \bigoplus_{k=1}^\ell Z^{(k)}$ and $X = \bigoplus_{k=1}^\ell X^{(k)}$ where $Z^{(k)}$ (resp. $X^{(k)}$) is the direct sum of the bars in Z (resp. X) with end-point b_k . Given a bar-to-bar monomorphism $f: Z \hookrightarrow X$, this induces monomorphisms $f^{(k)}: Z^{(k)} \hookrightarrow X^{(k)}$. We then observe that $f = \bigoplus_{k=1}^\ell f^{(k)}$, and so

$$\|\operatorname{coker} f\|_p = \left\| \left(\|\operatorname{coker} f^{(k)}\|_p \right)_{k=1, \dots, \ell} \right\|_p.$$

Since p -norms are nondecreasing with respect to the coordinate-wise order on $[0, \infty)^\ell$ (Section 2.6), proving that $\|\operatorname{coker} f_\varphi^{(k)}\|_p \leq \|\operatorname{coker} f^{(k)}\|_p$ for each $k \in \{1, \dots, \ell\}$ implies that $\|\operatorname{coker} f_\varphi\|_p \leq \|\operatorname{coker} f\|_p$.

Thus it suffices to prove the result in the case where the bars of Z and X all have the same end-point, which is what we assume for the rest of the proof. Denote by b_0 this common end-point and write $Z = \bigoplus_{i=1}^m K(a_i^z, b_0)$ and $X = \bigoplus_{j=1}^n K(a_j^x, b_0)$, where the a_i^z and a_j^x are in nondecreasing order. Define $a_i^z = b_0$ for $i \in \{m+1, \dots, n\}$. Then every bar-to-bar monomorphism $f: Z \hookrightarrow X$ has the form

$$f = \bigoplus_{i=1}^n (K(a_i^z, b_0) \hookrightarrow K(a_{\alpha(i)}^x, b_0)),$$

where $\alpha: \{1, \dots, n\} \rightarrow \{1, \dots, n\}$ is a permutation and $K(b_0, b_0)$ denotes the zero module. By Remark 3.2,

$$\operatorname{coker} f = \bigoplus_{i=1}^n K(a_{\alpha(i)}^x, a_i^z).$$

In particular, the bar-to-bar monomorphism induced by the canonical injection corresponds to the permutation $\alpha = \operatorname{id}$. For all $p \in [1, \infty)$, we then apply Corollary 3.13 to deduce that $\|\operatorname{coker} f_\varphi\|_p \leq \|\operatorname{coker} f\|_p$. The case $p = \infty$ follows by taking the limit (as in the proof of Theorem 3.14). \square

We now dualize the definitions and results for the case of epimorphisms. An epimorphism $f: Z \twoheadrightarrow X$ induces a canonical injection [BL15] from the multiset of bars of X to the multiset of bars of Z , where for all $a \in [0, \infty]$, the i^{th} longest bar of X with start-point a is sent to the i^{th} longest bar of Z with the same start-point.

Definition 3.21. Let Z and X be persistence modules such that there exists an epimorphism $Z \twoheadrightarrow X$, and fix barcode decompositions $Z = \bigoplus_{i=1}^m K(a_i^z, b_i^z)$ and $X = \bigoplus_{j=1}^n K(a_j^x, b_j^x)$. The induced matching of [BL15] then corresponds to a canonical injection $\psi: \{1, \dots, n\} \hookrightarrow \{1, \dots, m\}$. We define the **epimorphism induced by the canonical injection** ψ as the epimorphism $f_\psi: Z \twoheadrightarrow X$ given by

$$f_\psi = \bigoplus_{j=1}^n (K(a_{\psi(j)}^z, b_{\psi(j)}^z) \twoheadrightarrow K(a_j^x, b_j^x)) \oplus \bigoplus_{i \in \{1, \dots, m\} \setminus \operatorname{im} \psi} (K(a_i^z, b_i^z) \twoheadrightarrow 0).$$

As in the case of monomorphisms, given an epimorphism $f: Z \rightarrow X$, the associated bar-to-bar epimorphisms f_ψ and f_b (see Section 3.3) are not necessarily the same.

Corollary 3.22. *Let Z and X be two persistence modules such that there exists an epimorphism $Z \rightarrow X$. Then $\min_{f: Z \rightarrow X} \|\ker f\|_p = \|\ker f_\psi\|_p$ for all $p \in [1, \infty]$, where f_ψ is a bar-to-bar epimorphism induced by the canonical injection (Definition 3.21).*

Proof. This proof is dual to that of Corollary 3.20. By Theorem 3.16, it suffices to show the inequality $\|\ker f_\psi\|_p \leq \|\ker f\|_p$ for bar-to-bar epimorphisms $f: Z \rightarrow X$. Let $\{a_k\}_{k=1}^\ell$ be the set of distinct start-points of Z . We can decompose $Z = \bigoplus_{k=1}^\ell Z^{(k)}$ and $X = \bigoplus_{k=1}^\ell X^{(k)}$ where $Z^{(k)}$ (resp. $X^{(k)}$) is the direct sum of the bars in Z (resp. X) with start-point a_k . Given a bar-to-bar epimorphism $f: Z \rightarrow X$, this induces epimorphisms $f^{(k)}: Z^{(k)} \rightarrow X^{(k)}$ such that $f = \bigoplus_{k=1}^\ell f^{(k)}$, hence

$$\|\ker f\|_p = \left\| \left(\|\ker f^{(k)}\|_p \right)_{k=1, \dots, \ell} \right\|_p.$$

As in the proof of Corollary 3.20, it is sufficient to prove the claim for each $f^{(k)}$, hence for the rest of the proof we assume that the bars of Z and X all have the same start-point. Denote by a_0 this common start-point and write $Z = \bigoplus_{i=1}^m K(a_0, b_i^z)$ and $X = \bigoplus_{j=1}^n K(a_0, b_j^x)$, where the b_i^z and b_j^x are in nonincreasing order. Define $b_j^x = a_0$ for $i \in \{n+1, \dots, m\}$. Then every bar-to-bar epimorphism $f: Z \rightarrow X$ has the form

$$f = \bigoplus_{i=1}^m (K(a_0, b_i^z) \rightarrow K(a_0, b_{\alpha(i)}^x)),$$

where $\alpha: \{1, \dots, m\} \rightarrow \{1, \dots, m\}$ is a permutation and $K(a_0, a_0)$ denotes the zero module. By Remark 3.2,

$$\ker f = \bigoplus_{i=1}^m K(b_{\alpha(i)}^x, b_i^z).$$

In particular, the bar-to-bar epimorphism induced by the canonical injection corresponds to the permutation $\alpha = \text{id}$. For all $p \in [1, \infty)$, we then apply Corollary 3.13 to deduce that $\|\ker f_\varphi\|_p \leq \|\ker f\|_p$. The case $p = \infty$ follows by taking the limit. \square

4 Noise systems and Wasserstein pseudometrics

In this section we study algebraic Wasserstein pseudometrics between persistence modules. After introducing in Section 4.1 a generalization of the pseudometrics associated with a noise system, we study in Section 4.2 noise systems determined by p -norms of persistence modules and regular contours. Section 4.3 is devoted to the associated algebraic Wasserstein pseudometrics. For some choices of parameters, these pseudometrics have a combinatorial interpretation, as we show in Section 4.4. Finally, in Section 4.5 we present formulas to compute the algebraic Wasserstein pseudometric between persistence modules in some specific cases.

4.1 Pseudometrics associated to noise systems

Given a noise system \mathcal{S} and $p \in [1, \infty]$, in this section we will introduce pseudometrics $d_{\mathcal{S}}^p$ between persistence modules. These pseudometrics are a simple generalization to $p > 1$ of the

pseudometric associated to a noise system in [SCL⁺17] (see Section 2.4), where $p = 1$. Although the statements in this section hold true for tame functors indexed by $[0, \infty)^r$ for every positive natural number r , as in [SCL⁺17], we will limit the presentation to $r = 1$, since this is the setting of the following sections.

Definition 4.1. Let X and Y be persistence modules. A **span** of X, Y is a triplet (Z, f, g) with Z a persistence module and $f: Z \rightarrow X$ and $g: Z \rightarrow Y$ morphisms between persistence modules. A span of X, Y is therefore a diagram in \mathbf{Tame} of the form

$$X \xleftarrow{f} Z \xrightarrow{g} Y$$

Definition 4.2. Let X and Y be persistence modules, and let \mathcal{S} be a noise system. A span $X \xleftarrow{f} Z \xrightarrow{g} Y$ is called a $(\varepsilon_1, \varepsilon_2, \varepsilon_3, \varepsilon_4)$ -**span** if

$$\ker f \in \mathcal{S}_{\varepsilon_1}, \quad \text{coker } f \in \mathcal{S}_{\varepsilon_2}, \quad \ker g \in \mathcal{S}_{\varepsilon_3} \quad \text{and} \quad \text{coker } g \in \mathcal{S}_{\varepsilon_4}.$$

Definition 4.3. Let X and Y be persistence modules, and let \mathcal{S} be a noise system. For $p \in [1, \infty]$ and $\varepsilon \in [0, \infty)$, we say that X and Y are ε -**close in p -norm** $\|\cdot\|_p$ if there exists a $(\varepsilon_1, \varepsilon_2, \varepsilon_3, \varepsilon_4)$ -span $X \xleftarrow{f} Z \xrightarrow{g} Y$ for some $\varepsilon_1, \varepsilon_2, \varepsilon_3, \varepsilon_4 \in [0, \infty)$ such that $\|(\varepsilon_1, \varepsilon_2, \varepsilon_3, \varepsilon_4)\|_p \leq \varepsilon$. We define

$$d_{\mathcal{S}}^p(X, Y) := \inf \{ \varepsilon \in [0, \infty) \mid X \text{ and } Y \text{ are } \varepsilon\text{-close in } p\text{-norm} \},$$

adopting the convention $\inf \emptyset = \infty$.

Our next aim is to prove that $d_{\mathcal{S}}^p$ is a pseudometric on \mathbf{Tame} . We start by generalizing Proposition 8.5 in [SCL⁺17] to our current framework. Even if the generalization is not difficult, we include the proof to highlight how the properties of p -norms on \mathbb{R}^4 are used. We note that a similar result can be obtained for a larger family of subadditive functions on \mathbb{R}^4 which include p -norms (see [GNOW21], Section 2.1).

Proposition 4.4. *Let F, G, H be persistence modules. Assume that F and G are ε -close in p -norm, and that G and H are τ -close in p -norm. Then F and H are $(\varepsilon + \tau)$ -close in p -norm.*

Proof. By assumption there exists a $(\varepsilon_1, \varepsilon_2, \varepsilon_3, \varepsilon_4)$ -span $F \xleftarrow{f'} X \xrightarrow{f''} G$ with $\varepsilon_1, \varepsilon_2, \varepsilon_3, \varepsilon_4 \in [0, \infty)$ such that $\|(\varepsilon_1, \varepsilon_2, \varepsilon_3, \varepsilon_4)\|_p \leq \varepsilon$ and a $(\tau_1, \tau_2, \tau_3, \tau_4)$ -span $G \xleftarrow{g'} Y \xrightarrow{g''} H$ with $\tau_1, \tau_2, \tau_3, \tau_4 \in [0, \infty)$ such that $\|(\tau_1, \tau_2, \tau_3, \tau_4)\|_p \leq \tau$. Consider the following diagram, where the square is a pullback:

$$\begin{array}{ccccc} & & Z & & \\ & & \swarrow f & \searrow g & \\ & X & & & Y \\ & \swarrow f' & \searrow f'' & \swarrow g' & \searrow g'' \\ F & & G & & H \end{array}$$

By [SCL⁺17, Proposition 8.1], $\ker f \in \mathcal{S}_{\tau_1}$ and $\text{coker } f \in \mathcal{S}_{\tau_2}$, hence by [SCL⁺17, Proposition 8.2] $\ker f'f \in \mathcal{S}_{\varepsilon_1 + \tau_1}$ and $\text{coker } f'f \in \mathcal{S}_{\varepsilon_2 + \tau_2}$. By a similar argument, $\ker g''g \in \mathcal{S}_{\varepsilon_3 + \tau_3}$ and $\text{coker } g''g \in \mathcal{S}_{\varepsilon_4 + \tau_4}$. This proves that F and H are η -close in p -norm, where $\eta := \|(\varepsilon_1 + \tau_1, \varepsilon_2 + \tau_2, \varepsilon_3 + \tau_3, \varepsilon_4 + \tau_4)\|_p$. Our claim follows from the inequality

$$\|(\varepsilon_1 + \tau_1, \varepsilon_2 + \tau_2, \varepsilon_3 + \tau_3, \varepsilon_4 + \tau_4)\|_p \leq \|(\varepsilon_1, \varepsilon_2, \varepsilon_3, \varepsilon_4)\|_p + \|(\tau_1, \tau_2, \tau_3, \tau_4)\|_p \leq \varepsilon + \tau$$

which expresses the subadditivity of $\|\cdot\|_p$ and the hypotheses. \square

We are now ready to prove that $d_{\mathcal{S}}^p$ is a pseudometric on **Tame**.

Proposition 4.5. *Given $p \in [1, \infty]$ and a noise system \mathcal{S} , the function $d_{\mathcal{S}}^p$ in Definition 4.3 is a pseudometric on **Tame** (see Section 2.4).*

Proof. If $g: X \rightarrow Y$ is an isomorphism of persistence modules, the span $X \xleftarrow{\text{id}} X \xrightarrow{g} Y$ shows that $d_{\mathcal{S}}^p(X, Y) = 0$. For all persistence modules X and Y , the bijection between spans $X \xleftarrow{f} Z \xrightarrow{g} Y$ between X and Y and spans $Y \xleftarrow{g} Z \xrightarrow{f} X$ between Y and X implies that $d_{\mathcal{S}}^p(X, Y) = d_{\mathcal{S}}^p(Y, X)$. Proposition 4.4 shows that the triangle inequality holds true. \square

Remark 4.6. Given a noise system \mathcal{S} , the pseudometrics $d_{\mathcal{S}}^p$ for all $p \in [1, \infty]$ are strongly equivalent. Assuming $p \leq q$, for any pair of persistence modules X, Y we have

$$d_{\mathcal{S}}^q(X, Y) \leq d_{\mathcal{S}}^p(X, Y) \leq 4^{\left(\frac{1}{p} - \frac{1}{q}\right)} d_{\mathcal{S}}^q(X, Y),$$

as can be easily concluded from the properties on p -norms on \mathbb{R}^4 stated in Section 2.6.

4.2 p -norms of persistence modules and contours

The aim of this section is to introduce and study a generalization of the notion of p -norm of a persistence module (see Section 2.6) first introduced in [ST20], that coincides with the original definition if C is the standard contour (see Section 2.2).

Definition 4.7. Let C be a regular contour. For $p \in [1, \infty]$, define the (p, C) -**norm** of a persistence module $X \cong \bigoplus_{i=1}^k K(a_i, b_i)$ by

$$\|X\|_{p,C} := \begin{cases} \left(\sum_{i=1}^k \ell(a_i, b_i)^p \right)^{\frac{1}{p}} & \text{for } p \in [1, \infty), \\ \max\{\ell(a_i, b_i)\}_{i=1}^k & \text{for } p = \infty, \end{cases}$$

where $\ell(a_i, b_i)$ denotes the lifetime of the bar $K(a_i, b_i)$ with respect to C (see Section 2.2).

We see that $\|X\|_{p,C}$ does not depend on the choice of barcode decomposition for X . For $p \in [1, \infty]$ and $\varepsilon \in [0, \infty)$, consider the class of tame persistence modules

$$\mathcal{S}_{\varepsilon}^{p,C} := \{X \in \mathbf{Tame} \mid \|X\|_{p,C} \leq \varepsilon\},$$

and denote $\mathcal{S}^{p,C} := \{\mathcal{S}_{\varepsilon}^{p,C}\}_{\varepsilon \in [0, \infty)}$. If D is the standard contour (see Section 2.2), then $\ell(a_i, b_i) = b_i - a_i$ and we have $\|X\|_{p,D} = \|X\|_p$ and $\mathcal{S}^{p,D} = \mathcal{S}^p$. The main result in this subsection is showing that $\mathcal{S}^{p,C}$ is a noise system (see Section 2.3) whenever C is an action, for any $p \in [1, \infty]$. For the standard contour, this result together with Proposition 4.5 provide an algebraic proof that the algebraic p -Wasserstein distance introduced in [ST20] is a pseudometric, as will be later highlighted in Remark 4.20.

Given a contour C , the function $C(0, -): [0, \infty) \rightarrow [0, \infty)$ is nondecreasing. Hence it can be viewed as a functor from the poset category $[0, \infty)$ to itself. For any persistence module X , the composition of functors $T_C(X) := XC(0, -): [0, \infty) \rightarrow \text{vect}_K$ is a persistence module. As we will show, $T_C(X)$ is in **Tame** whenever X is in **Tame** and C is a regular contour (Corollary 4.11). The assignment $X \mapsto T_C(X)$ can be extended to a functor $T_C: \mathbf{Tame} \rightarrow \mathbf{Tame}$ sending a morphism $f: X \rightarrow Y$ of persistence modules to the morphism $T_C(f): T_C(X) \rightarrow T_C(Y)$ defined

as the natural transformation between $T_C(X)$ and $T_C(Y)$ whose component at $a \in [0, \infty)$ is $T_C(f)_a = f_{C(0,a)}: X_{C(0,a)} \rightarrow Y_{C(0,a)}$.

Since direct sums in **Tame** are defined pointwise (Section 2.1), if $\{X_i\}_{i \in I}$ is a finite collection of persistence modules and C is a contour, then $T_C(\bigoplus_{i \in I} X_i) \cong \bigoplus_{i \in I} T_C(X_i)$. Similarly, we show that the functor T_C preserves kernels and cokernels.

Proposition 4.8. *Let $0 \rightarrow X \rightarrow Y \rightarrow Z \rightarrow 0$ be an exact sequence in **Tame**, and let C be a regular contour. Then the sequence $0 \rightarrow T_C(X) \rightarrow T_C(Y) \rightarrow T_C(Z) \rightarrow 0$ is also exact.*

Proof. Exactness in **Tame** is defined pointwise: $0 \rightarrow X \rightarrow Y \rightarrow Z \rightarrow 0$ is exact if and only if $0 \rightarrow X_a \rightarrow Y_a \rightarrow Z_a \rightarrow 0$ is exact in vect_K , for every $a \in [0, \infty)$. As a consequence, $0 \rightarrow X_{C(0,b)} \rightarrow Y_{C(0,b)} \rightarrow Z_{C(0,b)} \rightarrow 0$ is exact in vect_K , for every $b \in [0, \infty)$, hence by definition the sequence $0 \rightarrow T_C(X) \rightarrow T_C(Y) \rightarrow T_C(Z) \rightarrow 0$ is exact. \square

Remark 4.9. As is clear from its proof, Proposition 4.8 holds for the precomposition of persistence modules by any increasing bijection of $[0, \infty)$ other than $C(0, -)$ for a regular contour C .

We now explain the relationship between the barcode decompositions of X and $T_C(X)$ when C is a regular contour.

Proposition 4.10. *Let C be a regular contour, and let ℓ be the associated lifetime function. Consider a bar $K(a, b)$. Then*

$$T_C(K(a, b)) \cong K(\ell(0, a), \ell(0, b)).$$

Proof. The functor $T_C(K(a, b)): [0, \infty) \rightarrow \text{vect}_K$ sends $c \leq d$ in $[0, \infty)$ to the linear function

$$K(a, b)_{C(0,c) \leq C(0,d)}: K(a, b)_{C(0,c)} \rightarrow K(a, b)_{C(0,d)},$$

which is the identity on K if $a \leq C(0, c) \leq C(0, d) < b$ and the zero function otherwise. Since C is regular, $\ell(0, -)$ is a strictly increasing function, hence the condition $a \leq C(0, c) \leq C(0, d) < b$ is equivalent to $\ell(0, a) \leq c \leq d < \ell(0, b)$. \square

Corollary 4.11. *Let X be a persistence module with barcode decomposition $\bigoplus_{i=1}^k K(a_i, b_i)$, and let C be a regular contour. Then $T_C(X) \cong \bigoplus_{i=1}^k K(\ell(0, a_i), \ell(0, b_i))$.*

Proof. We have

$$\begin{aligned} T_C(X) &\cong T_C\left(\bigoplus_{i=1}^k K(a_i, b_i)\right) \\ &\cong \bigoplus_{i=1}^k T_C(K(a_i, b_i)) \\ &= \bigoplus_{i=1}^k K(\ell(0, a_i), \ell(0, b_i)). \end{aligned} \quad (\text{by Proposition 4.10})$$

\square

In the rest of the article, we will focus on contours that are regular and actions (see Section 2.2). We prove here a simple but important property of such contours, and the associated lifetime function ℓ , which is used to prove the subsequent results.

Lemma 4.12. *If C is a regular contour and an action, then $\ell(a, c) = \ell(a, b) + \ell(b, c)$ for any $a \leq b \leq c$ in $[0, \infty)$.*

Proof. Let $a \leq b \leq c$. Using the definitions and the assumption that C is an action, we have $C(C(a, \ell(a, b)), \ell(b, c)) = C(a, \ell(a, b) + \ell(b, c))$. Again by definition, we observe that the left-hand side equals c , and that $c = C(a, \ell(a, b) + \ell(b, c))$ implies $\ell(a, c) = \ell(a, b) + \ell(b, c)$. \square

Proposition 4.13. *Let X be a persistence module, let $p \in [1, \infty]$, and let C be a regular contour that is an action. Then $\|X\|_{p,C} = \|T_C(X)\|_p$.*

Proof. Let $X \cong \bigoplus_{i=1}^k K(a_i, b_i)$. For any fixed $p \in [1, \infty)$, we have

$$\begin{aligned} \|T_C(X)\|_p &= \left(\sum_{i=1}^k (\ell(0, b_i) - \ell(0, a_i))^p \right)^{\frac{1}{p}} \\ &= \left(\sum_{i=1}^k \ell(a_i, b_i)^p \right)^{\frac{1}{p}} \\ &= \|X\|_{p,C}, \end{aligned}$$

where the first equality is by Corollary 4.11, the second one is by Lemma 4.12, and the third one is by definition of $\|\cdot\|_{p,C}$. The case $p = \infty$ is similar. \square

We are now ready to prove that $\mathcal{S}^{p,C}$, with C a regular contour that is an action, satisfies the axioms in the definition of noise system (see Section 2.3).

Lemma 4.14. *Let $0 \rightarrow X \rightarrow Y \rightarrow Z \rightarrow 0$ be an exact sequence in \mathbf{Tame} , and let C be a regular contour. Then $\|X\|_{p,C} \leq \|Y\|_{p,C}$ and $\|Z\|_{p,C} \leq \|Y\|_{p,C}$.*

For the standard contour, our statement coincides with Lemma 7.8 in [ST20], which is proven using the induced matchings [BL15] for monomorphisms and epimorphisms of persistence modules. Although structurally similar, our proof leverages bar-to-bar morphisms and our results of Section 3.

Proof. By Theorem 3.14, the existence of a monomorphism from X to Y implies the existence of a bar-to-bar monomorphism $f: X \hookrightarrow Y$. By Remark 3.2, there are barcode decompositions $X \cong \bigoplus_{i=1}^m X_i$ and $Y \cong \bigoplus_{j=1}^n Y_j$ with $m \leq n$ such that $f = \bigoplus_{i \in I} f_i \oplus \bigoplus_{j=m+1}^n h_j$, where each f_i is a monomorphism $X_i \hookrightarrow Y_i$ between bars and each h_j is the zero morphism $0 \rightarrow Y_j$. Now recall (see Section 2.1) that a monomorphism between bars $K(a, b)$ and $K(a', b')$ exists if and only if $a' \leq a$ and $b' = b$, and observe that this implies $\ell(a, b) \leq \ell(a', b')$ by monotonicity of contours. Considering the definition of $\|\cdot\|_{p,C}$, we see that every term in the expression for $\|X\|_{p,C}$ is upper bounded by a term in the expression for $\|Y\|_{p,C}$, implying that $\|X\|_{p,C} \leq \|Y\|_{p,C}$.

The proof of the inequality $\|Z\|_{p,C} \leq \|Y\|_{p,C}$ is obtained similarly, using Theorem 3.16 and dual arguments on epimorphisms. \square

Lemma 4.15. *Let $0 \rightarrow X \rightarrow Y \rightarrow Z \rightarrow 0$ be an exact sequence in \mathbf{Tame} , and let C be a regular contour that is an action. Then $\|Y\|_{p,C} \leq \|X\|_{p,C} + \|Z\|_{p,C}$.*

Proof. First, we prove the statement assuming that C is the standard contour. Let $0 \rightarrow X \xrightarrow{f} Y \xrightarrow{g} Z \rightarrow 0$ be a short exact sequence of persistence modules, and let us show that $\|Y\|_p \leq \|X\|_p + \|Z\|_p$. We consider the monomorphism f and observe that $Z \cong \operatorname{coker} f$ implies that Z and $\operatorname{coker} f$ have the same barcode decomposition, hence $\|Z\|_p = \|\operatorname{coker} f\|_p$. Theorem 3.14 tells us that, among all monomorphisms between two fixed persistence modules, the norm $\|\cdot\|_p$ of the cokernel is minimized by a bar-to-bar monomorphism. We therefore just need to prove that $\|Y\|_p \leq \|X\|_p + \|\operatorname{coker} f\|_p$, for any bar-to-bar monomorphism f between X and Y .

Let $\bigoplus_{i=1}^m X_i$ and $\bigoplus_{j=1}^n Y_j$ be barcode decompositions of X and Y , respectively. By Remark 3.2, if $f: X \rightarrow Y$ is a bar-to-bar monomorphism, then $m \leq n$ and, up to permutation of the Y_j , there are monomorphisms $f_i: X_i \rightarrow Y_i$ between bars such that $\operatorname{coker} f = \bigoplus_{i=1}^m \operatorname{coker} f_i \oplus \bigoplus_{j=m+1}^n Y_j$. We observe that, for each bar $Y_i = K(a_i, b_i)$ of Y with $i \in \{1, \dots, m\}$, there is a bar $X_i = K(a'_i, b_i)$ of X and a corresponding summand $\operatorname{coker} f_i$ of $\operatorname{coker} f$, which is a bar $K(a_i, a'_i)$ if $a_i < a'_i$, and it is the zero module if $a_i = a'_i$. Similarly, we observe that each bar $Y_j = K(a_j, b_j)$ of Y with $j \in \{m+1, \dots, n\}$ is also a bar of $\operatorname{coker} f$. By definition, $\|Y\|_p$ is the p -norm of the following element of \mathbb{R}^n :

$$(b_j - a_j)_{j \in \{1, \dots, n\}} = (((b_i - a'_i) + (a'_i - a_i))_{i \in \{1, \dots, m\}}, (b_j - a_j)_{j \in \{m+1, \dots, n\}}).$$

Then, by the triangular inequality of p -norms in \mathbb{R}^n , we have $\|Y\|_p \leq \|X\|_p + \|\operatorname{coker} f\|_p$, which completes the proof when C is the standard contour.

Let now C be any contour that is regular and an action. By Proposition 4.8, exactness of $0 \rightarrow X \rightarrow Y \rightarrow Z \rightarrow 0$ implies exactness of $0 \rightarrow T_C(X) \rightarrow T_C(Y) \rightarrow T_C(Z) \rightarrow 0$. Applying the previous part of the proof yields $\|T_C(Y)\|_p \leq \|T_C(X)\|_p + \|T_C(Z)\|_p$, which by Proposition 4.13 coincides with our claim. \square

For the standard contour, the statement of Lemma 4.15 is given in Remark 7.32 of [ST20]. However, to our knowledge, we provide the first algebraic proof of this inequality, which is the most difficult to show among the axioms of a noise system.

We can now prove the main result of this subsection.

Theorem 4.16. *For any $p \in [1, \infty]$ and any regular contour C that is an action, $\mathcal{S}^{p,C}$ is a noise system.*

Proof. We show that $\mathcal{S}^{p,C}$ satisfies all axioms of the definition of noise system (see Section 2.3). Since the norm $\|\cdot\|_{p,C}$ of the zero module 0 is zero, we have $0 \in \mathcal{S}_\varepsilon^{p,C}$, for all $\varepsilon \in [0, \infty)$. By definition of $\mathcal{S}^{p,C}$, it is clear that $\mathcal{S}_\tau^{p,C} \subseteq \mathcal{S}_\varepsilon^{p,C}$ whenever $\tau \leq \varepsilon$. Lemma 4.14 and Lemma 4.15 complete the proof, showing that $\mathcal{S}^{p,C}$ satisfies both conditions on short exact sequences of persistence modules. \square

Remark 4.17. For $p < \infty$, the noise system $\mathcal{S}^{p,C}$ is not closed under direct sums (Section 2.3), since $\|X \oplus Y\|_{p,C} = \|(\|X\|_{p,C}, \|Y\|_{p,C})\|_p$ by equation (2.2).

Remark 4.18. Let us briefly highlight the role of our hypotheses on contours, which are required to be regular and actions in Theorem 4.16. The regularity assumption ensures for instance that the associated lifetime function ℓ is well-defined, and that the functor T_C is an endofunctor on **Tame**. The weaker assumption that $C(0, -): [0, \infty) \rightarrow [0, \infty)$ is an increasing bijection is

sufficient to prove many results of this subsection, but we choose to assume the stronger condition of regularity to facilitate a comparison with the results of [CR20], observing in addition that many examples of regular contours can be found, for example the contours of distance type (Section 2.2) that are used in our experiments (see Section 5). The hypothesis that the considered contours are actions is necessary to obtain the main results of this subsection. In particular, it is important in Lemma 4.12, since otherwise we can only conclude $\ell(a, c) \leq \ell(a, b) + \ell(b, c)$ for any $a \leq b \leq c$. As is easy to show, Lemma 4.15 (and consequently Theorem 4.16) are not true if we remove the action hypothesis on contours. Consider for example the contour $C(a, \varepsilon) := a + \varepsilon^2$, which is regular but not an action [CR20]. Let r be a positive real number, and consider an exact sequence of bars $0 \rightarrow K(0, r^2) \rightarrow K(0, 2r^2) \rightarrow K(r^2, 2r^2) \rightarrow 0$. Assuming the claim of Lemma 4.15 holds for the contour C would imply $2^{\frac{1}{2}}r \leq 2^{\frac{1}{p}}r$ for any p , but the inequality holds if, and only if, $p \leq 2$.

4.3 Contours and algebraic Wasserstein distances

We now turn to considering the pseudometrics $d_{\mathcal{S}^{p,C}}^q$ associated (as in Section 4.1) with the noise systems $\mathcal{S}^{p,C}$ introduced in Section 4.2, for fixed $p, q \in [1, \infty]$ and a regular contour C that is an action. We also refer to these pseudometrics as **algebraic Wasserstein distances**. First, we show that the functor T_C introduced in Section 4.2 allows us to switch between a pseudometric $d_{\mathcal{S}^{p,C}}^q$ and the pseudometric $d_{\mathcal{S}^p}^q$ associated with the standard contour. More precisely, we show that T_C can be viewed as an isometry

$$T_C: (\mathbf{Tame}, d_{\mathcal{S}^{p,C}}^q) \rightarrow (\mathbf{Tame}, d_{\mathcal{S}^p}^q).$$

Let us recall that, if C is a regular contour, the function $C(0, -) : [0, \infty) \rightarrow [0, \infty)$ is an increasing bijection. Its inverse $\ell(0, -) := C^{-1}(0, -)$ is therefore an increasing bijection as well. Mimicking the definition of T_C given in Section 4.2, we can define a functor $T_\ell: \mathbf{Tame} \rightarrow \mathbf{Tame}$ given by precomposition by the increasing function $\ell(0, -)$. By Proposition 4.8, the functor $T_C: \mathbf{Tame} \rightarrow \mathbf{Tame}$ preserves kernels and cokernels, and T_ℓ has the same property by Remark 4.9. Furthermore, since $C(0, -)$ and $\ell(0, -)$ are inverse to each other, the compositions $T_C T_\ell$ and $T_\ell T_C$ are the identity functor $1_{\mathbf{Tame}}$ on \mathbf{Tame} .

To prove the following result, it is convenient to define the (p, q, C) -**cost** of a span $X \xleftarrow{f} Z \xrightarrow{g} Y$ of persistence modules as the element $c \in [0, \infty]$ defined by

$$c := \left\| \left(\|\ker f\|_{p,C}, \|\operatorname{coker} f\|_{p,C}, \|\ker g\|_{p,C}, \|\operatorname{coker} g\|_{p,C} \right) \right\|_q.$$

Proposition 4.19. *Let C be a regular contour that is an action, and let X, Y be persistence modules. Then*

$$d_{\mathcal{S}^{p,C}}^q(X, Y) = d_{\mathcal{S}^p}^q(T_C(X), T_C(Y)).$$

Proof. Let D denote the standard contour, and let us recall that the (p, D) -norm of a persistence module coincides with its p -norm (Section 4.2). We describe a correspondence between spans having the same cost, calculated with respect to (p, q, C) and (p, q, D) respectively.

Let $X \xleftarrow{f} Z \xrightarrow{g} Y$ be a span and let c be its (p, q, C) -cost. Applying the functor T_C , we

obtain the span $T_C(X) \xleftarrow{T_C(f)} T_C(Z) \xrightarrow{T_C(g)} T_C(Y)$, whose (p, q, D) -cost is

$$\begin{aligned} c' &= \left\| \left(\|\ker T_C(f)\|_p, \|\operatorname{coker} T_C(f)\|_p, \|\ker T_C(g)\|_p, \|\operatorname{coker} T_C(g)\|_p \right) \right\|_q \\ &= \left\| \left(\|T_C(\ker f)\|_p, \|T_C(\operatorname{coker} f)\|_p, \|T_C(\ker g)\|_p, \|T_C(\operatorname{coker} g)\|_p \right) \right\|_q \\ &= c, \end{aligned}$$

where the second equality holds because the functor T_C preserves kernels and cokernels, and the last equality holds by Proposition 4.13.

To prove the other direction of the correspondence, we start from a span $T_C(X) \xleftarrow{\varphi} T_C(Z) \xrightarrow{\psi} T_C(Y)$ whose (p, q, D) -cost is

$$k := \left\| \left(\|\ker \varphi\|_p, \|\operatorname{coker} \varphi\|_p, \|\ker \psi\|_p, \|\operatorname{coker} \psi\|_p \right) \right\|_q,$$

and we exhibit a span between X and Y whose (p, q, C) -cost equals k . Applying the functor T_ℓ , we obtain the span $X \xleftarrow{T_\ell(\varphi)} Z \xrightarrow{T_\ell(\psi)} Y$. To determine the (p, q, C) -cost of this span we observe that

$$\|\ker T_\ell(\varphi)\|_{p,C} = \|T_\ell(\ker \varphi)\|_{p,C} = \|T_C T_\ell(\ker \varphi)\|_p = \|\ker \varphi\|_p,$$

where the first equality holds because T_ℓ preserves kernels, the second equality is by Proposition 4.13, and the third equality holds because $T_C T_\ell = 1_{\mathsf{Tame}}$. Since similar equalities hold for $\operatorname{coker} T_\ell(\varphi)$, $\ker T_\ell(\psi)$ and $\operatorname{coker} T_\ell(\psi)$, the (p, q, C) -cost of the span $X \xleftarrow{T_\ell(\varphi)} Z \xrightarrow{T_\ell(\psi)} Y$ equals k . \square

Remark 4.20. Some of the pseudometrics between persistence modules that have been studied by other authors fall within the framework we have presented in this subsection and in Section 4.1. If C is a regular contour, the pseudometric denoted by d_C in [CR20, Sect. 6] coincide with our pseudometrics of the type $d_{S^\infty, C}^1$. In particular, for the standard contour (Section 2.2) the pseudometric $d_{S^\infty}^1$ coincides with the standard pseudometric already introduced in [SCL⁺17]. As we already mentioned, the algebraic pseudometrics introduced in [ST20, Sect. 7] are of the form $d_{S^p}^p$, thus coinciding with our pseudometrics with the choice $p = q$ and for the standard contour. In [GNOW21], the authors propose a framework to study distances on abelian categories which is equivalent to noise systems on abelian categories. The authors of [BSS23] also study distances on abelian categories, introducing the notion of exact weight, which is more general than noise systems as the first axiom on short exact sequences is relaxed. The so-called path metric associated with an exact weight is defined for zigzags of morphisms of arbitrary finite length, but for the particular case of path metrics on noise systems considering spans is sufficient. In this case, the path metric coincides with a pseudometric of the form d_S^1 . In particular, the path metric $d_{\mu\text{odim}}$ between persistence modules studied in [BSS23, Sect. 4] coincides with $d_{S^1}^1$ in our notations, while the p -Wasserstein distances introduced by the authors are different from our pseudometrics $d_{S^p, C}^q$.

4.4 Algebraic and combinatorial (p, C) -Wasserstein distances

In this subsection we consider Wasserstein distances between persistence diagrams. Here, we call these pseudometrics *combinatorial* Wasserstein distances, to distinguish them from the *algebraic*

pseudometrics $d_{\mathcal{S}^p, C}^q$ defined on the class of persistence modules. We introduce a new family of combinatorial Wasserstein distances, parametrized by $p, q \in [1, \infty]$ and a regular contour C that is an action, which generalize the Wasserstein distances commonly used in persistence theory. Finally, we prove isometry results involving the combinatorial Wasserstein distances and the algebraic Wasserstein distances $d_{\mathcal{S}^p, C}^q$ introduced in Section 4.2.

Let $U := \{(a, b) \in [0, \infty) \times [0, \infty) \mid a < b\}$ be a subset of the extended plane. A **persistence diagram** is a finite multiset $D = \{x_i\}_{i \in \mathcal{S}}$ of elements of U . Since D is a multiset, it may happen that $x_i = x_k$ for some $i \neq k$. The **diagonal** Δ of $[0, \infty)$ is the set $\Delta := \{(a, a) \mid a \in [0, \infty)\} \subset U$. For all $p \in [1, \infty]$, we denote by d_p the metric on U induced by the p -norm, defined by $d_p(x, y) := \|x - y\|_p$ for all $x, y \in U$, and we denote $d_p(x, \Delta) := \inf_{z \in \Delta} d_p(x, z)$. As is easy to show, if $x = (a, b)$, then $d_p(x, \Delta) = d_p(x, \bar{z})$ with $\bar{z} := (\frac{a+b}{2}, \frac{a+b}{2})$.

Let $D = \{x_i\}_{i \in \{1, \dots, m\}}$ and $D' = \{x'_j\}_{j \in \{1, \dots, n\}}$ be persistence diagrams. For any $p, q \in [1, \infty]$, the (p, q) -**Wasserstein distance** between D and D' is defined by

$$W_p^q(D, D') := \inf_{\alpha} \left\| \left(\left\| (d_p(x_i, x'_{\alpha(i)}))_{i \in I} \right\|_q, \left\| (d_p(x_i, \Delta))_{i \in \{1, \dots, m\} \setminus I} \right\|_q, \left\| (d_p(\Delta, x'_j))_{j \in \{1, \dots, n\} \setminus \alpha(I)} \right\|_q \right) \right\|_q,$$

where the infimum is over all injective functions $\alpha: I \rightarrow \{1, \dots, n\}$, with $I \subseteq \{1, \dots, m\}$.

Remark 4.21. We note that in the literature, the letters p and q are sometimes interchanged with respect to our notation of the parameters of Wasserstein distances between persistence diagrams. This is the case for instance in [ST20, Def. 2.7]. Our choice of notation is motivated by symmetry with the definition of algebraic Wasserstein distances, where a norm $\|\cdot\|_q$ is used to “aggregate” costs expressed with respect to a norm $\|\cdot\|_p$.

Let \mathcal{D} denote the set of all persistence diagrams. We define the function $\text{Dgm}: \mathbf{Tame} \rightarrow \mathcal{D}$ sending any persistence module X to the persistence diagram $\text{Dgm}(X)$ such that $X \cong \bigoplus_{(a,b) \in \text{Dgm}(X)} K(a, b)$, where we note that in the right-hand term each bar $K(a, b)$ appears the same number of times as the multiplicity of (a, b) in the multiset $\text{Dgm}(X)$. By virtue of the barcode decomposition theorem (Theorem 2.2), the function $\text{Dgm}: \mathbf{Tame} \rightarrow \mathcal{D}$ induces a bijection between the set \mathbf{Tame} / \sim of isomorphism classes of persistence modules and \mathcal{D} .

As proven in [ST20], if $p = q$ then the algebraic distance $d_{\mathcal{S}^p}^q$ between persistence modules coincides with the combinatorial distance W_p^q between the associated persistence diagrams.

Theorem 4.22 ([ST20]). *For any $p \in [1, \infty]$ and for any persistence modules X and Y we have*

$$d_{\mathcal{S}^p}^p(X, Y) = W_p^p(\text{Dgm}(X), \text{Dgm}(Y)).$$

It is worth observing that the equality of Theorem 4.22 does not hold when $p \neq q$. For example, we can consider the persistence modules

$$X = K(a_1, a_1 + \ell_1) \oplus K(a_2, a_2 + \ell_2) \oplus K(a_3, a_3 + \ell_3)$$

with ℓ_1, ℓ_2, ℓ_3 positive real numbers, and 0 , the zero module. Then, assuming $q < \infty$,

$$d_{\mathcal{S}^p}^q(X, 0) = \left(\left\| \left(\frac{\ell_1}{2}, \frac{\ell_2}{2}, \frac{\ell_3}{2} \right) \right\|_p^q + \left\| \left(\frac{\ell_1}{2}, \frac{\ell_2}{2}, \frac{\ell_3}{2} \right) \right\|_p^q \right)^{\frac{1}{q}}$$

(as we will prove in Lemma 4.23), while

$$W_p^q(\text{Dgm}(X), \text{Dgm}(0)) = \left(\left\| \left(\frac{\ell_1}{2}, \frac{\ell_1}{2} \right) \right\|_p^q + \left\| \left(\frac{\ell_2}{2}, \frac{\ell_2}{2} \right) \right\|_p^q + \left\| \left(\frac{\ell_3}{2}, \frac{\ell_3}{2} \right) \right\|_p^q \right)^{\frac{1}{q}}.$$

Given a contour C , we now define a function $\tau_C: U \rightarrow U$ as follows: for $x = (a, b) \in U$, we set $\tau_C(x) = (\ell(0, a), \ell(0, b))$, where $\ell(0, -)$ is the lifetime function associated with C (Section 2.2). If D is a persistence diagram, then by applying τ_C to each element of D we obtain a persistence diagram that we denote by $\tau_C(D)$. Hence, we have a function $\mathcal{D} \rightarrow \mathcal{D}$ which we denote again by τ_C , with a slight abuse of notation. If C is the standard contour, then τ_C is the identity function and in particular $\tau_C(D) = D$. Figure 1 illustrates a persistence diagram transformed by applying τ_C for a contour C of distance type.

Given a regular contour C , we define the **combinatorial (p, C) -Wasserstein distance** $W_{p,C}^p$ pulling back the pseudometric W_p^p via $\tau_C: \mathcal{D} \rightarrow \mathcal{D}$. Explicitly, for all persistence diagrams D and D' , we define $W_{p,C}^p(D, D') := W_p^p(\tau_C(D), \tau_C(D'))$. If C is regular and an action, then as a consequence of Corollary 4.11 we have $\text{Dgm}(T_C(X)) = \tau_C(\text{Dgm}(X))$, for every persistence module X . This implies, by virtue of Proposition 4.19 and Theorem 4.22, that

$$d_{\mathcal{S}^p, C}^p(X, Y) = W_{p,C}^p(\text{Dgm}(X), \text{Dgm}(Y)),$$

for all persistence modules X and Y .

To summarize, for any $p \in [1, \infty]$ and any contour C that is regular and an action, we have a commutative diagram of isometries

$$\begin{array}{ccc} (\text{Tame}, d_{\mathcal{S}^p, C}^p) & \xrightarrow{\text{Dgm}} & (\mathcal{D}, W_{p,C}^p) \\ T_C \downarrow & & \downarrow \tau_C \\ (\text{Tame}, d_{\mathcal{S}^p}^p) & \xrightarrow{\text{Dgm}} & (\mathcal{D}, W_p^p) \end{array}$$

4.5 Algebraic parametrized Wasserstein distances

The equivalence between algebraic and combinatorial Wasserstein distances for the case $p = q$, described in Section 4.4 or in [ST20] for the standard contour, implies that in general Wasserstein distances have no closed form. However, for specific classes of persistence modules the distance can be computed by a formula depending on the barcode decompositions of the persistence modules we are comparing. The focus of this section is to present such formulas for the exact computation of algebraic Wasserstein distances. To avoid distinguishing the cases $q < \infty$ and $q = \infty$ in stating the results of this subsection, for $q = \infty$ we set by convention $\frac{1}{q} = 0$ and $2^{\frac{1-q}{q}} = 2^{-1}$.

Lemma 4.23. *For all persistence modules X and all $p, q \in [1, \infty]$ we have*

$$d_{\mathcal{S}^p}^q(X, 0) = 2^{\frac{1-q}{q}} \|X\|_p.$$

Proof. Let $X = \bigoplus_{i=1}^k K(a_i, b_i)$ be a barcode decomposition of X , consider a persistence module of the form $Z = \bigoplus_{i=1}^k K(\frac{a_i+b_i}{2}, b_i)$ and a bar-to-bar morphism $f = \bigoplus_{i=1}^k f_i: Z \rightarrow X$, with

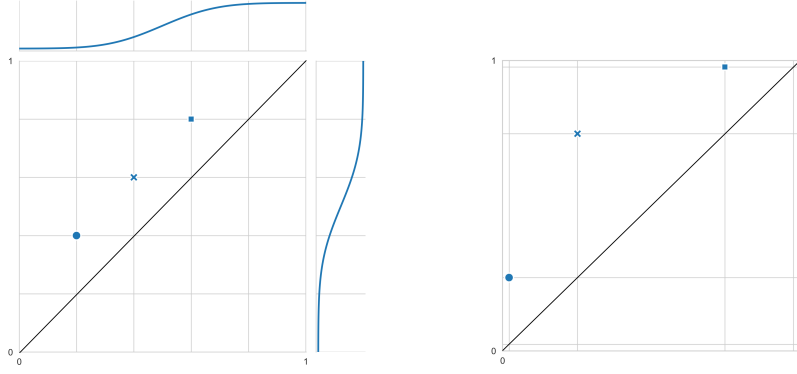


Figure 1: **Left:** A persistence diagram $D = \{(0.2, 0.4), (0.4, 0.6), (0.6, 0.8)\}$. A contour C of distance type parametrized by a Gaussian density ($\mu = 0.5, \sigma = 0.15$) is chosen and the corresponding function $f(x) = \ell(0, x)$ (i.e. the Gaussian cumulative distribution function) is shown above and to the right of the persistence diagram. **Right:** The transformed persistence diagram $\tau_C(D) = \{(\ell(0, 0.2), \ell(0, 0.4)), (\ell(0, 0.4), \ell(0, 0.6)), (\ell(0, 0.6), \ell(0, 0.8))\}$. The regular grid from the left diagram has also been transformed to illustrate how τ_C stretches the plane.

each $f_i: K(\frac{a_i+b_i}{2}, b_i) \rightarrow K(a_i, b_i)$ a monomorphism between bars. The existence of the span $X \xleftarrow{f} Z \rightarrow 0$ implies that X and 0 are $2^{\frac{1-q}{q}} \|X\|_p$ close in q -norm (Definition 4.3), proving that $d_{\mathcal{S}^p}^q(X, 0) \leq 2^{\frac{1-q}{q}} \|X\|_p$.

To prove the converse inequality, let us show that if $d_{\mathcal{S}^p}^q(X, 0) < \varepsilon$ then $2^{\frac{1-q}{q}} \|X\|_p < \varepsilon$. If $d_{\mathcal{S}^p}^q(X, 0) < \varepsilon$, then there exists a $(\varepsilon_1, \varepsilon_2, \varepsilon_3, 0)$ -span $X \xleftarrow{\varphi} Z \rightarrow 0$ for some $\varepsilon_1, \varepsilon_2, \varepsilon_3$ in $[0, \infty)$ such that $\|(\varepsilon_1, \varepsilon_2, \varepsilon_3)\|_q < \varepsilon$. Note that $X \leftarrow \text{im } \varphi \rightarrow 0$ is then a $(0, \varepsilon_2, \varepsilon_3, 0)$ -span. Consider the short exact sequence $\text{im } \varphi \hookrightarrow X \twoheadrightarrow \text{coker } \varphi$. Since $\text{coker } \varphi \in \mathcal{S}_{\varepsilon_2}^p$ and $\text{im } \varphi \in \mathcal{S}_{\varepsilon_3}^p$, by the third axiom of noise systems we get $X \in \mathcal{S}_{\varepsilon_2+\varepsilon_3}^p$, and so we get $\|X\|_p \leq \varepsilon_1 + \varepsilon_2$ by definition of \mathcal{S}^p . Furthermore, by inequalities (2.1) between p -norms on \mathbb{R}^2 , $\varepsilon_2 + \varepsilon_3 = \|(\varepsilon_2, \varepsilon_3)\|_1 \leq 2^{1-\frac{1}{q}} \|(\varepsilon_2, \varepsilon_3)\|_q < 2^{1-\frac{1}{q}} \varepsilon$. Therefore we have $\|X\|_p < 2^{1-\frac{1}{q}} \varepsilon$ or equivalently $2^{\frac{1-q}{q}} \|X\|_p < \varepsilon$. We conclude that $d_{\mathcal{S}^p}^q(X, 0) \geq 2^{\frac{1-q}{q}} \|X\|_p$, and therefore $d_{\mathcal{S}^p}^q(X, 0) = 2^{\frac{1-q}{q}} \|X\|_p$. \square

Remark 4.24. The formula $d_{\mathcal{S}^p}^q(X, 0) = 2^{\frac{1-q}{q}} \|X\|_p$ of Lemma 4.23 was already shown for the case $p = q$ in [ST20] by using the correspondence between combinatorial and algebraic Wasserstein distances.

The proof of Lemma 4.23 can be easily extended to the case of a regular contour C that is an action. In this case, we have

$$d_{\mathcal{S}^p, C}^q(X, 0) = d_{\mathcal{S}^p}^q(T_C(X), 0) = 2^{\frac{1-q}{q}} \|T_C(X)\|_p = 2^{\frac{1-q}{q}} \|X\|_{p, C}, \quad (4.1)$$

where the first equality holds by Proposition 4.19, the second by Lemma 4.23 and the third by Proposition 4.13. Similar arguments can be applied to all the results of this subsection. For exposition purposes we consider the case of the standard contour throughout the section and collect generalizations of the main results at the end of the subsection in Proposition 4.32.

Proposition 4.25. *Let X, Y, V be persistence modules. Then, for every $p, q \in [1, \infty]$,*

$$d_{\mathcal{S}^p}^q(X \oplus V, Y \oplus V) \leq d_{\mathcal{S}^p}^q(X, Y).$$

Proof. It suffices to observe that for any span $X \xleftarrow{f} Z \xrightarrow{g} Y$, the span $X \oplus V \xleftarrow{f \oplus 1} Z \oplus V \xrightarrow{g \oplus 1} Y \oplus V$ has the same cost. \square

Remark 4.26. Note that by considering $Y = 0$, Proposition 4.25 gives

$$d_{\mathcal{S}^p}^q(X \oplus V, V) \leq d_{\mathcal{S}^p}^q(X, 0) = 2^{\frac{1-q}{q}} \|X\|_p$$

The converse inequality $d_{\mathcal{S}^p}^q(X \oplus V, V) \geq d_{\mathcal{S}^p}^q(X, 0) = 2^{\frac{1-q}{q}} \|X\|_p$ does not hold in general, as illustrated in the following example. Consider $p = q = 2$, $X = K(0, 6)$ and $V = K(1, 5) \oplus K(2, 4)$. By Lemma 4.23 we have that $d_{\mathcal{S}^p}^q(X, 0) = \frac{1}{\sqrt{2}} \cdot 6 = \sqrt{18}$. However, $X \oplus V$ and $Y \oplus V$ are $\sqrt{6}$ -close via the following $(0, \sqrt{3}, \sqrt{3}, 0)$ -span

$$K(0, 6) \oplus K(1, 5) \oplus K(2, 4) \xleftarrow{f_1 \oplus f_2 \oplus f_3} K(1, 6) \oplus K(2, 5) \oplus K(3, 4) \xrightarrow{g_1 \oplus g_2 \oplus g_3} K(1, 5) \oplus K(2, 4) \oplus 0$$

implying that $d_{\mathcal{S}^p}^q(X \oplus V, Y \oplus V) \leq \sqrt{6} < \sqrt{18} = d_{\mathcal{S}^p}^q(X, Y)$. This example is based on the fact that given a span $X \xleftarrow{f} Z \xrightarrow{g} Y$ realizing the distance between X and Y , the span $X \oplus V \xleftarrow{f \oplus 1} Z \oplus V \xrightarrow{g \oplus 1} Y \oplus V$ not always is the one achieving the distance between $X \oplus V$ and $Y \oplus V$.

Let $\{K(a_i, b_i)\}_{i \in \{1, \dots, k\}}$ be a sequence of bars ordered non-decreasingly by length, that is, $b_1 - a_1 \leq b_2 - a_2 \leq \dots \leq b_k - a_k$. For $j \in \{1, \dots, k\}$, consider $Z := \bigoplus_{i=1}^j K(a_i, b_i)$ and $Y := \bigoplus_{i=j+1}^k K(a_i, b_i)$. The remainder of this section is devoted to proving that, in this case, $d_{\mathcal{S}^p}^q(Y \oplus Z, Y) = d_{\mathcal{S}^p}^q(Z, 0) = 2^{\frac{1-q}{q}} \|Z\|_p$. In Section 5, this result will be used for the computation of the stable rank of a persistence module with respect to $d_{\mathcal{S}^p}^q$.

Proposition 4.27. *Let \mathcal{S} be a noise system. For any $(\varepsilon_1, \varepsilon_2, \varepsilon_3, \varepsilon_4)$ -span $X \leftarrow Z \rightarrow Y$ of persistence modules there is a mono-epi $(0, \varepsilon_2, \varepsilon_3, 0)$ -span $X \leftarrow \text{im } f \rightarrow P$ such that $\text{rank}(P) \leq \text{rank}(Y)$.*

Proof. By Theorem 3.14 and Remark 3.2, if $U \hookrightarrow V$ is a monomorphism between persistence modules, then $\text{rank}(U) \leq \text{rank}(V)$, and similarly if $V \twoheadrightarrow U$ is an epimorphism, then $\text{rank}(U) \leq \text{rank}(V)$. Let $X \xleftarrow{f} Z \xrightarrow{g} Y$ be a $(\varepsilon_1, \varepsilon_2, \varepsilon_3, \varepsilon_4)$ -span of persistence modules, and consider the following diagram in Tame, where the square is a push-out:

$$\begin{array}{ccccc} & & Z & & \\ & & \swarrow f & \searrow g & \\ & \text{im } f & & \text{im } g & \\ j \swarrow & & & & \searrow i \\ X & & P & & Y \\ & \nearrow g' & \nwarrow f' & & \end{array}$$

Since f' is an epimorphisms and i is a monomorphism, $\text{rank}(P) \leq \text{rank}(\text{im } g) \leq \text{rank}(Y)$. We consider the span $X \xleftarrow{j} \text{im } f \xrightarrow{g'} P$. Clearly, the kernel of the corestriction $g: Z \twoheadrightarrow \text{im } g$ still belongs to $\mathcal{S}_{\varepsilon_3}$, and its cokernel is zero. Then, by Proposition 8.1 in [SCL⁺17], $\ker g' \in \mathcal{S}_{\varepsilon_3}$ and $\text{coker } g' = 0$. The kernel of j is 0, while its cokernel belongs to $\mathcal{S}_{\varepsilon_2}$, as it coincides with the cokernel of $f: Z \rightarrow X$. \square

Lemma 4.28. *Let $p, q \in [1, \infty]$, and let $[a_i, b_i]$ be nonempty intervals in $[0, \infty)$, for $i \in \{1, \dots, j\}$. The function $\gamma: \prod_{i=1}^j [a_i, b_i] \rightarrow [0, \infty)$ defined by*

$$\gamma(x_1, \dots, x_j) := \left\| \left(\| (x_1 - a_1, \dots, x_j - a_j) \|_p, \| (b_1 - x_1, \dots, b_j - x_j) \|_p \right) \right\|_q$$

has a global minimum at $(\frac{a_1+b_1}{2}, \dots, \frac{a_j+b_j}{2})$.

Proof. The function γ is continuous with a compact domain, so it admits a global minimum by the extreme value theorem. Moreover, it is convex because norms are convex functions.

Write $a = (a_1, \dots, a_j)$, $b = (b_1, \dots, b_j)$ and $x = (x_1, \dots, x_j)$ in \mathbb{R}^j . Since $\gamma(x) = \gamma(a + b - x)$ for every x , the function γ is invariant under point reflection through $\frac{a+b}{2}$. By convexity, we conclude that $\frac{a+b}{2}$ is a global minimum of γ . \square

Proposition 4.29. *Let $X = \bigoplus_{i=1}^k K(a_i, b_i)$, with the bars ordered non-decreasingly by length. Let $j \in \{1, \dots, k\}$, and let $p, q \in [1, \infty]$. Then, any persistence module Y with $\text{rank}(Y) \leq \text{rank}(X) - j$ is such that*

$$d_{\mathcal{S}^p}^q(X, Y) \geq 2^{\frac{1-q}{q}} \left\| \bigoplus_{i=1}^j K(a_i, b_i) \right\|_p.$$

Proof. We prove the claim by contradiction. Suppose that there exists a persistence module Y such that $\text{rank}(Y) \leq \text{rank}(X) - j$ and

$$d_{\mathcal{S}^p}^q(X, Y) < 2^{\frac{1-q}{q}} \left\| \bigoplus_{i=1}^j K(a_i, b_i) \right\|_p.$$

By definition, there exists a span $X \xleftarrow{f} Z \xrightarrow{g} Y$ such that

$$\left\| \left(\| \ker f \|_p, \| \text{coker } f \|_p, \| \ker g \|_p, \| \text{coker } g \|_p \right) \right\|_q < 2^{\frac{1-q}{q}} \left\| \bigoplus_{i=1}^j K(a_i, b_i) \right\|_p. \quad (4.2)$$

By Proposition 4.27 we can assume (possibly after replacing Y with a persistence module of smaller or equal rank) that the span above is mono-epi, that is, of the form $X \xleftarrow{f} Z \xrightarrow{g} Y$. By Theorems 3.14 and 3.16, we can moreover assume that f and g are bar-to-bar morphisms.

Thus, we can consider a barcode decomposition $Z = \bigoplus_{i=1}^k Z_i$, with some of the Z_i possibly zero, and a barcode decomposition $Y = \bigoplus_{i=1}^k Y_i$, with at least j of the Y_i equal to zero by assumption, together with morphisms between bars $K(a_i, b_i) \xleftarrow{f_i} Z_i \xrightarrow{g_i} Y_i$ such that $f = \bigoplus_{i=1}^k f_i$ and $g = \bigoplus_{i=1}^k g_i$. Let $I \subseteq \{1, \dots, k\}$, with $|I| \geq j$, be the subset of the indices i such that $Y_i = 0$. For every $i \in I$, we have $K(a_i, b_i) \xleftarrow{f_i} Z_i \xrightarrow{g_i} 0$, with $Z_i = K(x_i, b_i)$ for some $a_i \leq x_i \leq b_i$, where $K(b_i, b_i)$ denotes the zero module. Since $\ker f = \bigoplus_{i=1}^k \ker f_i$ and $\text{coker } f = \bigoplus_{i=1}^k \text{coker } f_i$, by Remark 3.2 we observe that $\bigoplus_{i \in I} K(a_i, x_i)$ is a direct summand of $\text{coker } f$, and similarly that $\bigoplus_{i \in I} K(x_i, b_i)$ is a direct summand of $\ker g$, which gives

$$\begin{aligned} \| \text{coker } f \|_p &\geq \| \bigoplus_{i \in I} K(a_i, x_i) \|_p = \| (x_i - a_i)_{i \in I} \|_p, \\ \| \ker g \|_p &\geq \| \bigoplus_{i \in I} K(x_i, b_i) \|_p = \| (b_i - x_i)_{i \in I} \|_p. \end{aligned}$$

If $b_i < \infty$ for all $i \in I$, it is easy to show using Lemma 4.28 that the cost of the span is

$$\left\| \left(\| \text{coker } f \|_p, \| \ker g \|_p \right) \right\|_q \geq 2^{\frac{1-q}{q}} \| (b_i - a_i)_{i \in I} \|_p = 2^{\frac{1-q}{q}} \left\| \bigoplus_{i \in I} K(a_i, b_i) \right\|_p,$$

and the same inequality clearly holds if $b_i = \infty$ for some $i \in I$. However, since $|I| \geq j$, the right-hand side of the inequality cannot be smaller than

$$2^{\frac{1-q}{q}} \left\| (b_i - a_i)_{i \in \{1, \dots, j\}} \right\|_p = 2^{\frac{1-q}{q}} \left\| \bigoplus_{i=1}^j K(a_i, b_i) \right\|_p,$$

and this contradicts (4.2). \square

Proposition 4.30. *Let $X = \bigoplus_{i=1}^k K(a_i, b_i)$, with the bars ordered non-decreasingly by length. Let $j \in \{1, \dots, k\}$, and let $Y = \bigoplus_{i=j+1}^k K(a_i, b_i)$ (with $Y = 0$ when $j = k$). Then, for all $p, q \in [1, \infty]$,*

$$d_{\mathcal{S}^p}^q(X, Y) = 2^{\frac{1-q}{q}} \left\| \bigoplus_{i=1}^j K(a_i, b_i) \right\|_p. \quad (4.3)$$

Proof. Since $\text{rank}(Y) = \text{rank}(X) - j$, Proposition 4.29 gives us the inequality

$$d_{\mathcal{S}^p}^q(X, Y) \geq 2^{\frac{1-q}{q}} \left\| \bigoplus_{i=1}^j K(a_i, b_i) \right\|_p.$$

To prove the other direction, it is enough to exhibit a span between X and Y with cost equal to the right-hand side of (4.3). We construct a mono-epi and bar-to-bar span $X \xleftarrow{f} Z \xrightarrow{g} Y$ as follows. Let

$$Z := \bigoplus_{i=1}^j K\left(\frac{a_i+b_i}{2}, b_i\right) \oplus \bigoplus_{i=j+1}^k K(a_i, b_i),$$

and let $f = \bigoplus_{i=1}^k f_i$ and $g = \bigoplus_{i=1}^k g_i$ with

$$f_i = \begin{cases} K\left(\frac{a_i+b_i}{2}, b_i\right) \hookrightarrow K(a_i, b_i) & \text{if } 1 \leq i \leq j \\ K(a_i, b_i) \xrightarrow{\text{id}} K(a_i, b_i) & \text{if } j+1 \leq i \leq k, \end{cases}$$

$$g_i = \begin{cases} K\left(\frac{a_i+b_i}{2}, b_i\right) \rightarrow 0 & \text{if } 1 \leq i \leq j \\ K(a_i, b_i) \xrightarrow{\text{id}} K(a_i, b_i) & \text{if } j+1 \leq i \leq k. \end{cases}$$

Recalling Remark 3.2, we observe that $\ker f = \text{coker } g = 0$ and $\|\text{coker } f\|_p = \|\ker g\|_p = \left\| \left(\frac{b_i - a_i}{2} \right)_{i \in \{1, \dots, j\}} \right\|_p$. The cost $\left\| \left(\|\text{coker } f\|_p, \|\ker g\|_p \right) \right\|_q$ of this span is therefore as claimed. \square

In the final part of this subsection we generalize some results from the case of the standard contour to the case of any regular contour C that is an action.

Definition 4.31. Let C be a regular contour, and let $X = \bigoplus_{i=1}^k K(a_i, b_i)$. We say that (the barcode decomposition of) X has **bars ordered non-decreasingly by lifetime** if $\ell(a_1, b_1) \leq \ell(a_2, b_2) \leq \dots \leq \ell(a_k, b_k)$, where ℓ denotes the lifetime function associated with C (see Section 2.2).

Proposition 4.32. *Let C be a regular contour and an action, and let $p, q \in [1, \infty]$. Let $X = \bigoplus_{i=1}^k K(a_i, b_i)$, with bars ordered non-decreasingly by lifetime, and let $j \in \{1, \dots, k\}$. Then, for all persistence modules Y ,*

1. *if $\text{rank}(Y) \leq \text{rank}(X) - j$, then*

$$d_{\mathcal{S}^p, C}^q(X, Y) \geq 2^{\frac{1-q}{q}} \left\| \bigoplus_{i=1}^j K(a_i, b_i) \right\|_{p, C};$$

2. *if $Y = \bigoplus_{i=j+1}^k K(a_i, b_i)$ (with the convention $Y = 0$ when $j = k$), then*

$$d_{\mathcal{S}^p, C}^q(X, Y) = 2^{\frac{1-q}{q}} \left\| \bigoplus_{i=1}^j K(a_i, b_i) \right\|_{p, C}.$$

Proof. The first statement follows from

$$\begin{aligned} d_{\mathcal{S}^p, C}^q(X, Y) &= d_{\mathcal{S}^p}^q(T_C(X), T_C(Y)) \\ &\geq 2^{\frac{1-q}{q}} \left\| \bigoplus_{i=1}^j T_C(K(a_i, b_i)) \right\|_p \\ &= 2^{\frac{1-q}{q}} \left\| \bigoplus_{i=1}^j K(a_i, b_i) \right\|_{p, C} \end{aligned}$$

where we are using in sequence Proposition 4.19, Proposition 4.29 (observing that the length of a bar $T_C(K(a, b))$ coincides with the lifetime $\ell(a, b)$ of $K(a, b)$, see Proposition 4.10), and Proposition 4.13. The second statement is proven similarly, using Proposition 4.30. \square

5 Wasserstein stable ranks: computations and stability

In Section 4 it was shown that the Wasserstein distances $d_{\mathcal{S}^p, C}^q$ are pseudometrics on Tame . They can therefore be used in the framework of hierarchical stabilization (see Section 2.5) to produce stable invariants of persistence modules. The focus of this section is on one type of such invariants, the **Wasserstein stable ranks**, which are the hierarchical stabilization of the rank function with respect to Wasserstein distances $d_{\mathcal{S}^p, C}^q$. Denoting $d_{\mathcal{S}^p, C}^q$ by d , the stability result for stable ranks (Proposition 2.5) states that for every pair of persistence modules X and Y

$$d(X, Y) \geq d_{\bowtie}(\widehat{\text{rank}}_d(X), \widehat{\text{rank}}_d(Y)).$$

In the case where $p = q$ and C is the standard contour, combining the above inequality with the stability results of [ST20] gives several stability results of Wasserstein stable ranks with respect to perturbation of the original data. In particular, [ST20, Theorem 4.8] expresses stability with respect to sublevel set filtrations of monotone functions on cellular complexes, [ST20, Theorem 5.1] expresses stability with respect to the construction of cubical complexes from grey scale images, and [ST20, Theorem 5.9], expresses stability with respect to Wasserstein distance between point clouds when using the Vietoris-Rips construction.

In order to use the Wasserstein stable ranks in applications, it is important to be able to efficiently compute them as well as distances between them. In this section we use computations of Wasserstein distances from Section 4 to derive a formula for the Wasserstein stable rank and propose a convenient formulation of the interleaving distance between stable ranks.

Having defined a rich family of Wasserstein distances $d_{\mathcal{S}^p, C}^q$, it is natural to ask whether we can in a supervised learning context search for an optimal distance for a problem at hand. Choosing a suitable parametrization of a contour and leveraging the simple expression of the interleaving distance between Wasserstein stable ranks, in Section 5.3 we set up a simple metric learning problem with the aim of observing the interaction between the parameter p and the parameters related to the contour C within the learning. Preliminary results on the optimization of only a contour in a metric learning framework are presented in [Gäv18].

5.1 Computation of the stable rank with Wasserstein distances

The results of this subsection provide explicit formulas to compute the stable rank with respect to the Wasserstein distances $d_{\mathcal{S}^p, C}^q$ introduced in Section 4. We begin by showing that the computation of the stable rank of a persistence module X can be reduced to the computation of the stable rank of the submodule X' formed by all finite bars of X . As in the previous section, if $q = \infty$ we set by convention $\frac{1}{q} = 0$ and $2^{\frac{1-q}{q}} = 2^{-1}$.

Proposition 5.1. *Let $X = \bigoplus_{i=1}^k K(a_i, b_i)$, and let d denote the pseudometric $d_{\mathcal{S}^p, C}^q$, for some $p, q \in [1, \infty]$ and a regular contour C that is an action. Let $I := \{i \in \{1, \dots, k\} \mid b_i < \infty\}$, $J := \{i \in \{1, \dots, k\} \mid b_i = \infty\}$, and consider the submodules $X' := \bigoplus_{i \in I} K(a_i, b_i)$ and $X'' := \bigoplus_{i \in J} K(a_i, b_i)$ such that $X = X' \oplus X''$. Then $\widehat{\text{rank}}_d(X) = \widehat{\text{rank}}_d(X') + \text{rank}(X'')$.*

Proof. We prove that, for any $t \in [0, \infty)$, we have $\widehat{\text{rank}}_d(X)(t) = \widehat{\text{rank}}_d(X')(t) + \text{rank}(X'')$. Let $r := \widehat{\text{rank}}_d(X')(t)$, meaning that there exists a persistence module Y' such that $\text{rank}(Y') = r$ and $d(X', Y') \leq t$. By Proposition 4.32(2), since X'' contains only infinite bars, $d(X' \oplus X'', Y' \oplus X'') = d(X', Y')$. Furthermore, $\text{rank}(Y' \oplus X'') = r + \text{rank}(X'')$. This proves $\widehat{\text{rank}}_d(X) \leq \widehat{\text{rank}}_d(X') + \text{rank}(X'')$.

To prove the converse inequality, let $t \in [0, \infty)$ and let $n := \widehat{\text{rank}}_d(X)(t)$, meaning that there is a persistence module Y such that $\text{rank}(Y) = n$ and $d(X, Y) \leq t$. We can assume that X has bars ordered non-decreasingly by lifetime (Definition 4.31). By Proposition 4.32, we can take $Y = \bigoplus_{i=k-n+1}^k K(a_i, b_i)$, and we know that $d(X, Y) = 2^{\frac{1-q}{q}} \left\| \bigoplus_{i=1}^{k-n} K(a_i, b_i) \right\|_{p,C} \leq t$, which implies that $n \geq \text{rank}(X'')$. We can consider X' and its $m := n - \text{rank}(X'')$ bars with greatest lifetime, and define $Y' := \bigoplus_{i=\text{rank}(X')-m+1}^{\text{rank}(X')} K(a_i, b_i)$. Using Proposition 4.32 again and observing that $\text{rank}(X') - m = k - n$, we have

$$d(X', Y') = 2^{\frac{1-q}{q}} \left\| \bigoplus_{i=1}^{\text{rank}(X')-m} K(a_i, b_i) \right\|_{p,C} = d(X, Y),$$

so $\widehat{\text{rank}}_d(X')(t) \leq \text{rank}(Y') = n - \text{rank}(X'')$. Rearranging the terms of this inequality, we obtain $\widehat{\text{rank}}_d(X) \geq \widehat{\text{rank}}_d(X') + \text{rank}(X'')$. \square

Corollary 5.2. *Let $X = \bigoplus_{i=1}^k K(a_i, b_i)$, and let d denote the pseudometric $d_{S^p,C}^q$, for some $p, q \in [1, \infty]$ and a regular contour C that is an action. Then,*

$$\lim_{t \rightarrow \infty} \widehat{\text{rank}}_d(X)(t) = |\{i \in \{1, \dots, k\} \mid b_i = \infty\}|.$$

Proof. We apply Proposition 5.1, observing that $\widehat{\text{rank}}_d(X')(t) = 0$ for a sufficiently large $t \in [0, \infty)$ since $d(X', 0)$ is finite by equation (4.1). \square

We now prove a formula to compute the stable rank of a persistence module X . By Proposition 5.1, we can restrict to the case in which X has only finite bars. First, we consider the case $p < \infty$.

Proposition 5.3. *Let $p \in [1, \infty)$ and $q \in [1, \infty]$, let C be a regular contour that is an action, and let d denote the pseudometric $d_{S^p,C}^q$. Let $X = \bigoplus_{i=1}^k K(a_i, b_i)$, with $b_i < \infty$ for every $i \in \{1, \dots, k\}$ and assume that bars in the barcode decomposition of X are ordered non-decreasingly by lifetime (Definition 4.31). Then, there exist real numbers $0 = t_0 < t_1 < t_2 < \dots < t_k$ such that the stable rank function $\widehat{\text{rank}}_d(X): [0, \infty) \rightarrow [0, \infty)$ is constant on the intervals $[t_0, t_1)$, $[t_1, t_2)$, \dots , $[t_{k-1}, t_k)$, $[t_k, \infty)$, and*

$$\widehat{\text{rank}}_d(X)(t_j) = \text{rank}(X) - j,$$

for every $j \in \{0, 1, \dots, k\}$. Furthermore,

$$t_j = 2^{\frac{1-q}{q}} \left\| \bigoplus_{i=1}^j K(a_i, b_i) \right\|_{p,C} = 2^{\frac{1-q}{q}} \|(\ell(a_1, b_1), \dots, \ell(a_j, b_j))\|_p$$

for every $j \in \{1, \dots, k\}$, where ℓ is the lifetime function associated with C .

Proof. For every $j \in \{1, \dots, k\}$, by Proposition 4.32 $Y_j := \bigoplus_{i=j+1}^k K(a_i, b_i)$ is the closest persistence module to X (in the pseudometric $d_{S^p,C}^q$) such that $\text{rank}(Y_j) = \text{rank}(X) - j$. We have

$$d_{S^p,C}^q(X, Y_j) = 2^{\frac{1-q}{q}} \left\| \bigoplus_{i=1}^j K(a_i, b_i) \right\|_{p,C} =: t_j,$$

and we observe that $0 = t_0 < t_1 < t_2 < \dots < t_k$ as a consequence of the assumption $p < \infty$. \square

In particular, when $p < \infty$, the value of the piecewise constant function $\widehat{\text{rank}}_d(X)$ can only decrease by 1 at every discontinuity point t_j . For $p = \infty$, the stable rank has a slightly different behavior. Even though we can define the sequence of real numbers $(t_j)_j$ as in Proposition 5.3, we only have $0 = t_0 \leq t_1 \leq t_2 \leq \dots \leq t_k$ instead of strict inequalities. Letting s_m denote the m^{th} smallest value in $\{t_j\}_j$ we obtain a sequence $0 = s_0 < s_1 < s_2 < \dots < s_{k'}$ such that the stable rank with respect to the pseudometric $d := d_{\mathcal{S}^\infty, C}^q$ is constant on the intervals $[s_0, s_1), \dots, [s_{k'}, \infty)$, taking the values

$$\widehat{\text{rank}}_d(X)(s_m) = \text{rank}(X) - \max\{j \mid t_j = s_m\}.$$

An explicit formula for the stable rank in the case $p = \infty$ and $q = 1$ was first given in [CR20].

Remark 5.4. We observe that for a persistence module X of rank k , once the k bars in the barcode decomposition of X have been ordered non-decreasingly by lifetime, the complexity of computing the discontinuity points of the the Wasserstein stable rank using Proposition 5.3 is linear in k . Therefore the computational complexity of the Wasserstein stable rank is $O(k \log k)$, determined by the complexity of the sorting algorithm to order the bars non-decreasingly by lifetime.

5.2 Interleaving distance between stable ranks

The aim of this subsection is to propose a convenient expression for the interleaving distance (Section 2.5) between two non-increasing piecewise constant functions. We assume functions to take only finitely many values, that is the case of stable ranks which will be the object of our study. Let $f, g: [0, \infty) \rightarrow [0, \infty)$ be non-increasing piecewise constant functions. If $\lim_{t \rightarrow \infty} f(t) \neq \lim_{t \rightarrow \infty} g(t)$, then $d_{\infty}(f, g) = \infty$. For the computation of the interleaving distance we can therefore assume that the functions f and g have the same limit value and denote it by L . Given a non-increasing piecewise constant function $f: [0, \infty) \rightarrow [0, \infty)$ with limit value L , we define the non-increasing piecewise constant function $f^{-1}: [L, \infty) \rightarrow [0, \infty)$ with values $f^{-1}(y) := \inf\{t \mid f(t) \leq y\}$. If in addition the function f is right-continuous, then $f^{-1}(y) = \min\{t \mid f(t) \leq y\}$. We observe that for every right-continuous non-increasing piecewise constant function f we have $f^{-1}(f(t)) \leq t$ for all t , and equality holds if t is a discontinuity point of f . Moreover, $f(f^{-1}(y)) \leq y$ for all $y \geq L$, and equality holds if $y \in \text{im } f$. Our focus in this subsection will be on the discontinuity points $\{t_i\}$ of f and on the values in $\text{im } f$, rather than on the full domain and codomain of f , thus justifying our use of the notation f^{-1} .

Proposition 5.5. *Consider two right-continuous non-increasing piecewise constant functions $f, g: [0, \infty) \rightarrow [0, \infty)$ having the same limit value L . Using the notation introduced above, we have:*

$$d_{\infty}(f, g) = \|f^{-1} - g^{-1}\|_{\infty}.$$

Proof. Let us define the following subset of $[0, \infty)$,

$$A(f, g) := \{\varepsilon \in [0, \infty) \mid f(t) \geq g(t + \varepsilon) \text{ and } g(t) \geq f(t + \varepsilon), \text{ for all } t \in [0, \infty)\}.$$

Remember that, by definition, $d_{\infty}(f, g) = \inf A(f, g)$.

We first prove that $d_{\bowtie}(f, g) \geq \|f^{-1} - g^{-1}\|_{\infty}$. Let $\varepsilon \in A(f, g)$. Then, for all $y \geq L$, we have $y \geq f(f^{-1}(y)) \geq g(f^{-1}(y) + \varepsilon)$. Composing by the non-increasing function g^{-1} and recalling that $g^{-1}(g(t)) \leq t$ for all t , we obtain $f^{-1}(y) + \varepsilon \geq g^{-1}(y)$. We have thus shown that $g^{-1}(y) - f^{-1}(y) \leq \varepsilon$, for all $y \geq L$ and $\varepsilon \in A(f, g)$, which implies $g^{-1}(y) - f^{-1}(y) \leq d_{\bowtie}(f, g)$, for all $y \geq L$. By symmetry in the roles of f and g , we conclude that $|g^{-1}(y) - f^{-1}(y)| \leq d_{\bowtie}(f, g)$, for all $y \geq L$.

We now prove that $d_{\bowtie}(f, g) \leq \|f^{-1} - g^{-1}\|_{\infty}$ by showing that $\varepsilon := \|f^{-1} - g^{-1}\|_{\infty}$ is in $A(f, g)$. For any $t \in [0, \infty)$, there exists $y \geq L$ such that $f(t) = f(f^{-1}(y))$ (which implies $f^{-1}(y) \leq t$), as it is enough to take $y = f(t)$. Since $g^{-1}(y) \leq f^{-1}(y) + \varepsilon$ by definition of ε , $f^{-1}(y) \leq t$, and g is non-increasing, we get the following inequalities:

$$f(t) = y \geq g(g^{-1}(y)) \geq g(f^{-1}(y) + \varepsilon) \geq g(t + \varepsilon).$$

By symmetry, we also get $g(t) \geq f(t + \varepsilon)$, and we conclude that $\varepsilon \in A(f, g)$. \square

If f is the Wasserstein stable rank of a persistence module, by Proposition 5.3 it is right-continuous, which implies that the values of f^{-1} can be computed as minima and correspond the discontinuity points of f . If we denote by $\{t_1, \dots, t_k\}$ the set of discontinuity points of f and set $t_0 := 0$, then $f^{-1}(f(t_i)) = t_i$ for $i \in \{0, \dots, k\}$, and these values are sufficient to encode f^{-1} . Indeed, by definition $f^{-1}(y) = t_i$ for $f(t_i) \leq y < f(t_{i+1})$ and $i \in \{0, \dots, k\}$, and $f^{-1}(y) = t_0$ for $y \leq f(t_0)$. This implies that the interleaving distance between two stable ranks f and g can be realized as the L^{∞} norm between two finite vectors. Explicitly, evaluating f^{-1} and g^{-1} on the union of the discontinuity points of these two functions, one obtains finite vectors \hat{f}^{-1} and \hat{g}^{-1} such that $\|\hat{f}^{-1} - \hat{g}^{-1}\|_{\infty} = \|f^{-1} - g^{-1}\|_{\infty}$. By using the characterization in Proposition 5.3 of discontinuity points of Wasserstein stable ranks, the interleaving distance between the Wasserstein stable ranks of persistence modules $X = \bigoplus_{i=1}^n K(a_i, b_i)$ and $Y = \bigoplus_{i=1}^m K(c_i, d_i)$, both with bars ordered non-decreasingly by lifetime, can be written as the L^{∞} norm of the vector $(\hat{f}_i^{-1} - \hat{g}_i^{-1})_{i=0, \dots, \min(n, m)}$ with components:

$$\hat{f}_i^{-1} - \hat{g}_i^{-1} = 2^{\frac{1-q}{q}} (\|\ell(a_1, b_1), \dots, \ell(a_{n-i}, b_{n-i})\|_p - \|\ell(c_1, d_1), \dots, \ell(c_{m-i}, d_{m-i})\|_p). \quad (5.1)$$

Remark 5.6. For two persistence modules X and Y both of rank k , the complexity of computing the interleaving distance is dominated by the sorting of the bars in the respective barcode decompositions of X and Y , since forming the vector as in (5.1) and computing its L^{∞} norm can be done linearly in k . The computational complexity of the interleaving distance between Wasserstein stable ranks is thus $O(k \log k)$.

Example 5.7. Consider a persistence module $Y = \bigoplus_{i=1}^3 K(a_i, b_i)$ with bars ordered non-decreasingly by lifetime and $X = K(a_0, b_0) \oplus Y$ such that $\varepsilon := \ell(a_0, b_0) \leq \ell(a_1, b_1)$. By using the formula (5.1) and observing that

$$\|(\ell(a_0, b_0), \dots, \ell(a_i, b_i))\|_p - \|(\ell(a_1, b_1), \dots, \ell(a_i, b_i))\|_p \leq \ell(a_0, b_0)$$

for $i \in \{1, 2, 3\}$ by properties (2.1) and (2.2) of p -norms, we see that the interleaving distance between $\widehat{\text{rank}}_d(X)$ and $\widehat{\text{rank}}_d(Y)$ with $d = d_{\mathcal{S}p, C}^q$ is given by $2^{\frac{1-q}{q}} \varepsilon$. Note that by Proposition 4.32 we know $d_{\mathcal{S}p, C}^q(X, Y) = 2^{\frac{1-q}{q}} \|K(a_0, b_0)\|_{p, C} = 2^{\frac{1-q}{q}} \varepsilon$. Therefore in this case the interleaving

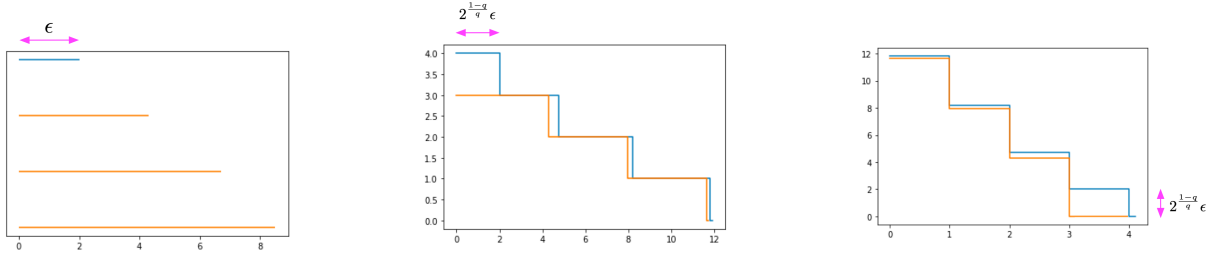


Figure 2: Schematic representation of the computation of the interleaving distance in Example 5.7. **Left:** Barcode decomposition of Y in orange and bar $K(a_0, b_0)$ in blue. **Middle:** Stable ranks computed with standard contour, $q = 1$ and $p = 2$. The functions $\widehat{\text{rank}}_d(X)$ and $\widehat{\text{rank}}_d(Y)$ are represented in blue and orange, respectively. **Right:** Inverse stable ranks for the computation of interleaving distance, with $\widehat{\text{rank}}_d^{-1}(X)$ in blue and $\widehat{\text{rank}}_d^{-1}(Y)$ in orange. The interleaving distance between stable ranks can be computed as $\|\widehat{\text{rank}}_d^{-1}(X) - \widehat{\text{rank}}_d^{-1}(Y)\|_\infty = 2^{\frac{1-q}{q}} \epsilon$, illustrated with the pink arrow.

distance between stable ranks with respect to Wasserstein distance coincides with the Wasserstein distance between X and Y . Note however that this is not always the case. The Wasserstein stable ranks of X and Y with respect to $d_{Sp,C}^q$, with parameters $q = 1$, $p = 2$ and C the standard contour, are shown in Figure 2, together with their “inverse” functions which are used for the computation of the interleaving distance.

Let us keep denoting $d_{Sp,C}^q$ by d . It follows from triangle inequality and Lemma 4.23 that:

$$d(X, Y) \geq 2^{\frac{1-q}{q}} \left| \|X\|_p - \|Y\|_p \right|.$$

However this inequality can be refined by

$$d(X, Y) \geq d_{\bowtie}(\widehat{\text{rank}}_d(X), \widehat{\text{rank}}_d(Y)) \geq 2^{\frac{1-q}{q}} \left| \|X\|_p - \|Y\|_p \right|,$$

where the first inequality is given by the stability theorem of hierarchical stabilization (Proposition 2.5) and the second inequality is provided by the characterization of interleaving distances between stable ranks in Proposition 5.5. An example where the second inequality is strict is provided by Example 5.7 for $p > 1$, while an example where this is an equality is provided in the case $Y = 0$ by Lemma 4.23. A simple example in which the first inequality is strict is provided instead by $X = K(0, 1)$, $Y = K(0, 2)$ and $q = 2$.

Remark 5.8. Since stable ranks are measurable functions $[0, \infty) \rightarrow [0, \infty)$, there are many pseudometrics to compare them other than the interleaving distance d_{\bowtie} . In particular, one can consider the standard L^p -pseudometrics, here denoted by $d_p(f, g) := (\int_0^\infty |f(t) - g(t)|^p dt)^{\frac{1}{p}}$. As shown in [CR20, Prop. 2.1], the stability theorem of hierarchical stabilization implies the following bounds for d_p :

$$c d(X, Y)^{\frac{1}{p}} \geq d_p(\widehat{\text{rank}}_d(X), \widehat{\text{rank}}_d(Y)),$$

for any persistence modules X and Y , where $c := \max\{\text{rank}(X), \text{rank}(Y)\}$ and d denotes any pseudometric between persistence modules. In this article we have chosen to work with the interleaving distance between Wasserstein stable ranks because of the strong stability result, expressed as a 1-Lipschitz condition. Lipschitz stability for Wasserstein distances other than W_1 can not be obtained for example by considering linear representations of persistence diagrams

[HKNU17, AEK⁺17, CWRW15, KFH17, RHBK15] as proved in Theorem 6.3 in [ST20]. The trade-off between stability and the possibility of exploiting a Banach or Hilbert space structure is still to be explored.

5.3 Metric learning

We have defined distances $d_{\mathcal{S}^p, C}^q$ between persistence modules, parametrized by q , p and by a contour C , and computable stable rank invariants with corresponding interleaving distances. These distances can be pulled back to compare persistence modules in Tame via the function $\widehat{\text{rank}}_d$, with $d = d_{\mathcal{S}^p, C}^q$. Recalling that the stable ranks depend on the pseudometric $d_{\mathcal{S}^p, C}^q$, we now turn to the question of how to choose p and C . The optimization of the parameter q is not relevant, since it determines a constant multiplicative factor to the distance of each pair of persistence modules. We thus fix $q = 1$ for a direct comparison with the original framework of noise systems.

For brevity, we write $d := d_{\mathcal{S}^p, C}^1$ and $d_{\bowtie, p, C}(X, Y) := d_{\bowtie}(\widehat{\text{rank}}_d(X), \widehat{\text{rank}}_d(Y))$. The field of metric learning provides a variety of loss functions suited for different machine learning problems. For example, if we consider a simple binary classification problem we have a dataset of persistence modules $\{X_i\}_{i \in I}$ and the index set I is partitioned into two sets A and B , to represent the labeling. For this problem, a loss function (from [ZW19]), designed to yield small intra-class distances and large inter-class distances can be formulated as:

$$\mathcal{L} = \frac{\sum_{i, j \in A} (d_{\bowtie, p, C}(X_i, X_j))^2}{\sum_{i \in A, j \in I} (d_{\bowtie, p, C}(X_i, X_j))^2} + \frac{\sum_{i, j \in B} (d_{\bowtie, p, C}(X_i, X_j))^2}{\sum_{i \in B, j \in I} (d_{\bowtie, p, C}(X_i, X_j))^2} \quad (5.2)$$

In order to proceed we need to choose a family of contours that is practically searchable when minimizing the loss function above. We work with contours of distance type which are parametrized by densities (see Section 2.2). In turn, in order to use gradient optimization methods, we want the densities to be parametrized by a finite real-valued parameter vector. To this aim we choose as densities unnormalized Gaussian mixtures $f(x) = \sum_{i=1}^k \lambda_i \mathcal{N}(x | \mu_i, \sigma_i)$ for some chosen k , where \mathcal{N} is Gaussian with mean μ_i and standard deviation σ_i , and $\lambda_1 = 1$.

In summary, the metric learning problem amounts to minimizing the loss function with respect to a parameter vector $\theta \in \mathbb{R}^{3k}$, i.e. $\theta = (\mu_1, \dots, \mu_k, \sigma_1, \dots, \sigma_k, \lambda_2, \dots, \lambda_k, p)$, designed to learn conjointly the parameter p and the parameters of the contour of the algebraic Wasserstein distance. The loss function is a simple function of the pairwise interleaving distances between Wasserstein stable ranks of persistence modules in the dataset. As can be seen in Proposition 5.5 and the expression (5.1), the interleaving distance between stable ranks is the L^∞ norm of differentiable functions with respect to θ and is therefore differentiable almost everywhere with respect to θ , implying the same behavior for the loss function. Hence the metric learning problem is amenable to gradient-based optimization methods such as gradient descent.

6 Examples of analyses with Wasserstein stable ranks

In a first experiment, we show how varying the parameter p affects the distance space of the Wasserstein stable ranks and can serve as a way to weight the importance of long bars versus short bars, for a set of synthetic persistence modules. In a second experiment, we illustrate on a

real-world dataset how learning the parameter p together with the parameters of a contour can lead to more discriminative Wasserstein stable ranks in a classification problem.

6.1 Synthetic data

A straightforward way to apply persistent homology in the context of computer vision is to construct a complex (e.g. cubical complex) from the grid of pixels constituting an image. The complex is then filtered based on the grayscale intensity of the pixels (or based on the color channels for color images).

It is easy to see that, in this context, what should be considered as signal versus noise in a barcode representation of the data is highly dependent on the application. For example, for classification of handwritten digits from the MNIST dataset [GT19, TNVL21] the dominant topological features are often the most discriminative (for instance the existence of a 1-dimensional cycle may be enough to distinguish between digits 0 and 1). On the other hand, in biomedical imaging [CHLS18, QTT⁺19] pathological states can translate into images with irregularities or lack of homogeneity, associated with high numbers of short-lived components as observed in [GHMM19].

Inspired by these applications, we construct two much simpler synthetic datasets of images and associated persistence modules, with the goal of illustrating the effect of choosing the parameter p when using Wasserstein stable ranks. The parameter q is set to 1 and the contour is fixed to be the standard contour. In other words, we study the effect of the parameter p on how the function $\widehat{\text{rank}}_d$, with $d = d_{\mathcal{S}^p}^1$, maps persistence modules onto the space of stable ranks, endowed with the interleaving distance. Each dataset is composed of 100 images together with their class label, A or B. Each image is composed of one block of high-intensity pixels and a number of blocks of low-intensity pixels (while the size of the pixel blocks does not have a direct impact on the following persistent homology analysis, the high-intensity block is made larger for visual clarity, see Figures 3, 4). The images are represented as cubical complexes on which super-level set filtration is performed and we analyze the H_0 barcodes obtained from this process. Since we use pixel intensity $[0, 255]$ and super-level sets are used, the resulting filtration scale is $[255, -\infty)$. This is capped to the minimum pixel value, 0, and transformed as $255 - x$ to obtain a filtration scale $[0, 255]$ as can be seen in the barcodes in Figures 3, 4.

- In Dataset 1 the pixels in the high-intensity block have slightly higher intensity in images from class A (uniformly distributed between 245 and 255) compared to images of class B (between 200 and 210). The low-intensity blocks however follow the same distribution for images of both classes (the number of blocks is uniformly distributed between 50 and 100 and the intensity is between 1 and 10). Sample images and barcodes are shown in Figure 3.
- In Dataset 2 on the other hand, the intensity of the high-intensity blocks follows the same distribution for both classes (uniformly distributed between 100 and 255). The number of low-intensity blocks however follows a different distribution for Class A (between 20 and 30) and Class B (between 120 and 130). Their intensity is the same for both classes (between 1 and 10). Sample images and barcodes are shown in Figure 4.

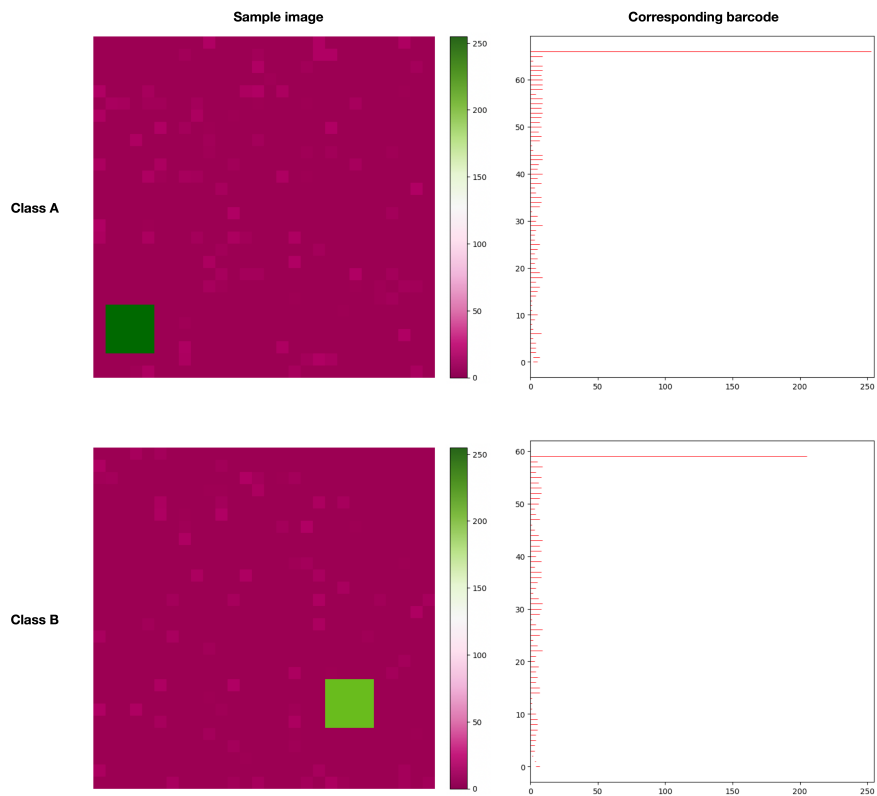


Figure 3: Dataset 1. **Left:** Sample images from classes A and B. **Right:** H_0 barcodes corresponding to the sample images.

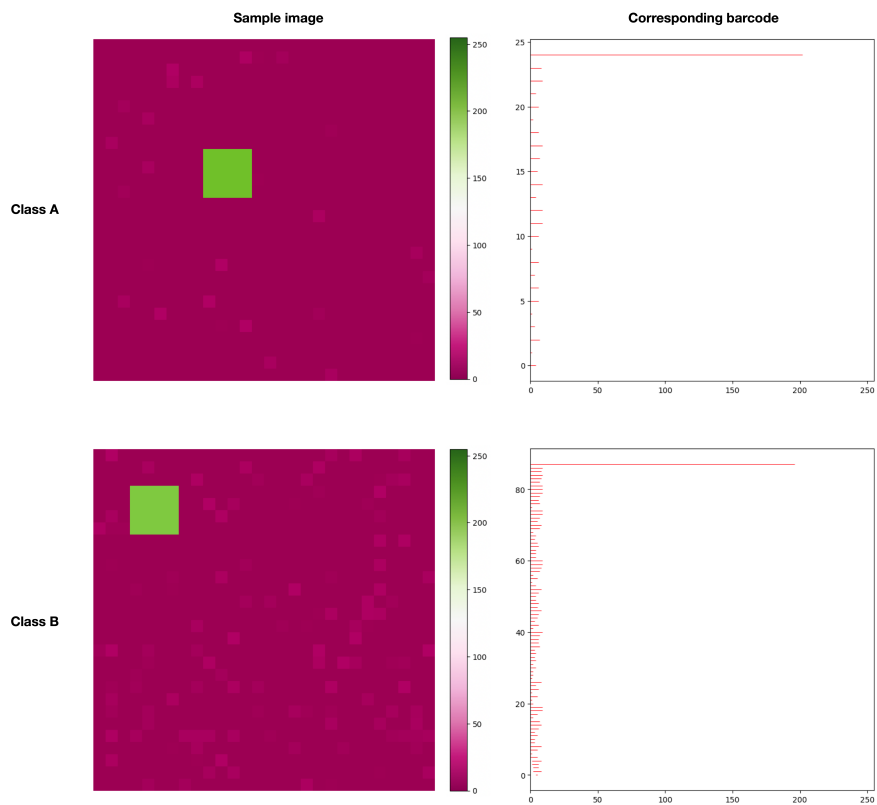


Figure 4: Dataset 2. **Left:** Sample images from classes A and B. **Right:** H_0 barcodes corresponding to the sample images.

This construction defines distributions of barcodes where barcode features (i.e. length of longest bar or number of bars in a given length range) are expected to be statistically distinct or indistinguishable. In terms of the barcodes, for Dataset 1 the signal is by construction the single dominant topological feature (the long bar, whose length follows statistically different distributions between classes) while the noise is composed of the numerous short bars (corresponding to low intensity blocks, for which the number and intensity follows the same distribution in both classes).

In accordance with the intuition, for Dataset 1, choosing a value of $p = \infty$ when generating the stable ranks effectively “denoises” the barcodes and organizes the space of Wasserstein stable ranks in a way where stable ranks of the same class are close to each other in interleaving distance but far from elements of the other class. Stable ranks corresponding to $p = 1$ however fail to organize the corresponding distance space in this clear-cut way, being too sensitive to the noisy short bars in the barcodes. To illustrate this effect, in Figure 5 we show the hierarchical clustering (with average linkage, similar results were observed for complete and single linkage) corresponding to the distance spaces of Wasserstein stable ranks for $p = 1$ and $p = \infty$.

On the contrary, for Dataset 2 the signal is by construction the number of short bars (whose number follows statistically different distributions) while the noise is the single long bar (generated by blocks following the same distribution for both classes). In this case a choice of $p = 1$ organizes the space of stable ranks such that elements of the same class cluster together, while $p = \infty$, being too sensitive to the (for this dataset) noisy long bar, fails to do so. This is illustrated in Figure 6.

While with the parameters used for the generation of our artificial datasets the effect of changing p on the structure of the distance space is clear, some class-based structure remains on a small scale, also when choosing $p = \infty$. By increasing the amount of noise it is however possible to induce e.g. a nearest neighbor classifier to perform arbitrary poorly for the $p = \infty$ while still distinguishing the classes for $p = 1$ (and vice versa for Dataset 1).

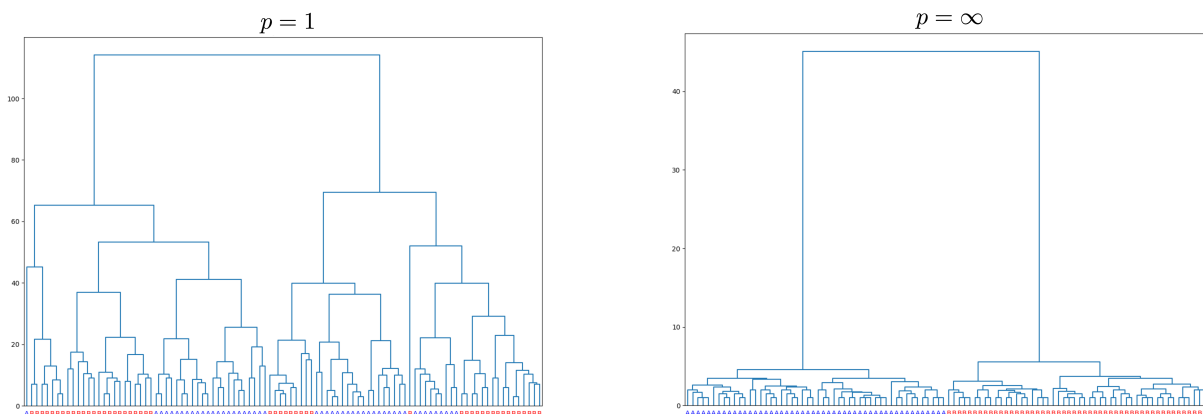


Figure 5: Dataset 1. Hierarchical clustering on the Wasserstein stable ranks for $p = 1$ (left) and $p = \infty$ (right) with respect to the interleaving distance. The leaves (stable ranks in the dataset) are labeled and colored according to their class.

The choice of the parameter value p , which we have demonstrated can have a large impact, is essentially related to the underlying distance between persistence modules. Using Wasserstein-stable invariants however has computational advantages, facilitates learning the right parameters

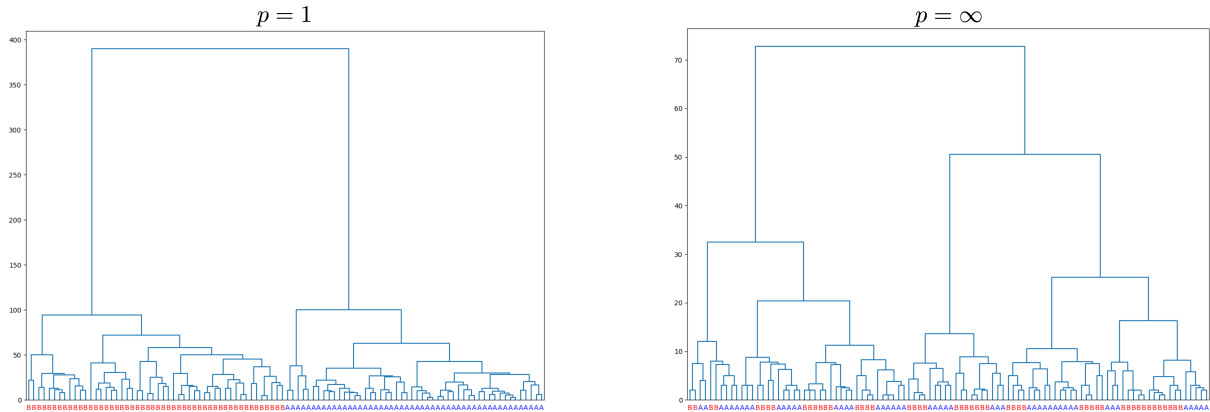


Figure 6: Dataset 2. Hierarchical clustering on the Wasserstein stable ranks for $p = 1$ (left) and $p = \infty$ (right) with respect to the interleaving distance. The leaves (stable ranks in the dataset) are labeled and colored according to their class.

for a particular problem and allows for a richer use of machine learning methods as we illustrate in the next section on a real-world dataset.

6.2 Brain artery data

In [BZM⁺10] a dataset of brain artery trees corresponding to 97 subjects aged 18 to 72 is introduced. Each data point is modeled as a tree embedded in \mathbb{R}^3 . In [BMM⁺16] the dataset is further analyzed with persistent homology. To be able to apply a sublevel set filtration on the tree, a real-valued function is defined on the vertices as the height of the vertex in the 3D-embedding. This is extended to a function on the edges by taking the maximum value of the weights of the vertices connected by the edge. After applying persistent homology, each tree is represented by a vector containing the sorted lengths of the 100 longest bars in a barcode decomposition of the corresponding persistence module. This feature is further used to demonstrate, among other things, an age effect of brain artery structure, by showing that the projection of the vectors on the first principal component of the dataset is correlated with age.

The authors note that using vectors of sorted length was computationally more feasible than computing Wasserstein distances between the persistence diagrams and they are more amenable to statistical analysis. In addition, the authors observed that it was not necessary to use the whole vector of lengths to establish the correlation and in fact the topological features of medium length, rather than the longest ones, were the most discriminatory.

Analyzing the dataset with stable ranks offers computational and statistical advantages. Moreover, for this problem where the discriminative information is not contained in the most persistent feature, considering other distances than the bottleneck ($p = \infty$) and more generally tuning the parameter p might be beneficial. Finally, combining the tuning of the parameter p with a contour might increase the power of the method. Indeed the parameter p and the contour, intuitively are related to different features of a persistence barcode: while the parameter p globally weights the importance of long versus short bars as illustrated in Section 6.1, the contour allows to focus on the most informative filtration scales.

While we also study age effects of brain artery structure, we choose to binarize the problem by creating two classes of similar size: *young* ($age < 45$, 50 subjects) and *old* ($age \geq 45$, 47

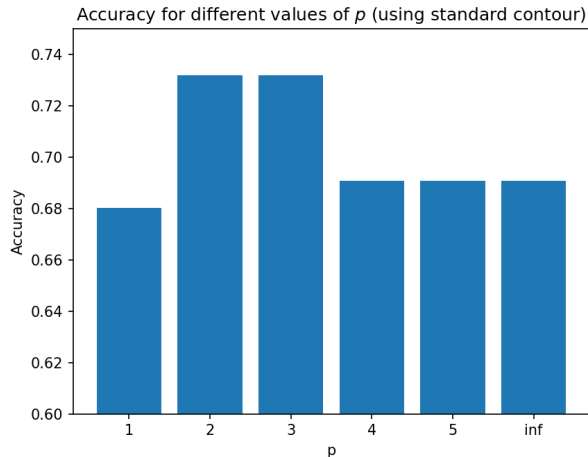


Figure 7: Accuracy on the brain artery problem using distances between stable ranks and KNN, for standard contour and different values of p .

subjects) and treat the problem as a classification.

We start by studying the effect of varying p alone. We compute the distances between Wasserstein stable ranks with standard contour. We classify the samples in the distance space thus obtained by using the k -nearest neighbors algorithm [PVG⁺11] (the parameter k is chosen in a cross-validation procedure). Repeating this for various values of p we observe a difference in the resulting accuracy, plotted in Figure 7, with the highest values obtained for p in the medium range (2 – 3). This is in line with the conclusion in [BMM⁺16] that the highest persistent features alone have a small distinguishing power, while medium sized bars reflect variations in brain artery trees within subject of different ages. In [BMM⁺16] only the length of bars in a barcode is used to compare barcodes of different classes. With our features parametrized by p and a contour C , we can take into consideration both the length of bars and their position in the parameter space.

We therefore next turn to the problem of learning the contour of the stable ranks as well. We use the metric learning method described in Section 5.3. Using leave-one-out cross-validation (LOOCV), for each training fold we learn the metric that optimally separates training samples from the two classes by minimizing the loss defined in (5.2). We then classify using KNN in the obtained distance space.

For the metric learning, the contours are parametrized by densities which are unnormalized Gaussian mixtures with two components. The loss function is implemented in PyTorch [PGM⁺19]. After a random initialization of the parameters, projected gradient descent (to respect the constraints $p \geq 1, \lambda_i, \sigma_i > 0$) with momentum is used to achieve a lower loss. An example of an optimization on a training fold over 25000 iterations is shown in Figure 8. The average and standard deviation of the optimized parameters, over the LOOCV folds can instead be found in Table 1.

The metric learning is effective in finding distances that improve the classification performance: running the optimization problem not only decreases the loss but also increases the corresponding classification accuracy (as is seen in Figure 8 in the top left plot), from accuracies between 44.3% and 71.1% (for 10 random initializations of the parameters in Table 1) to an

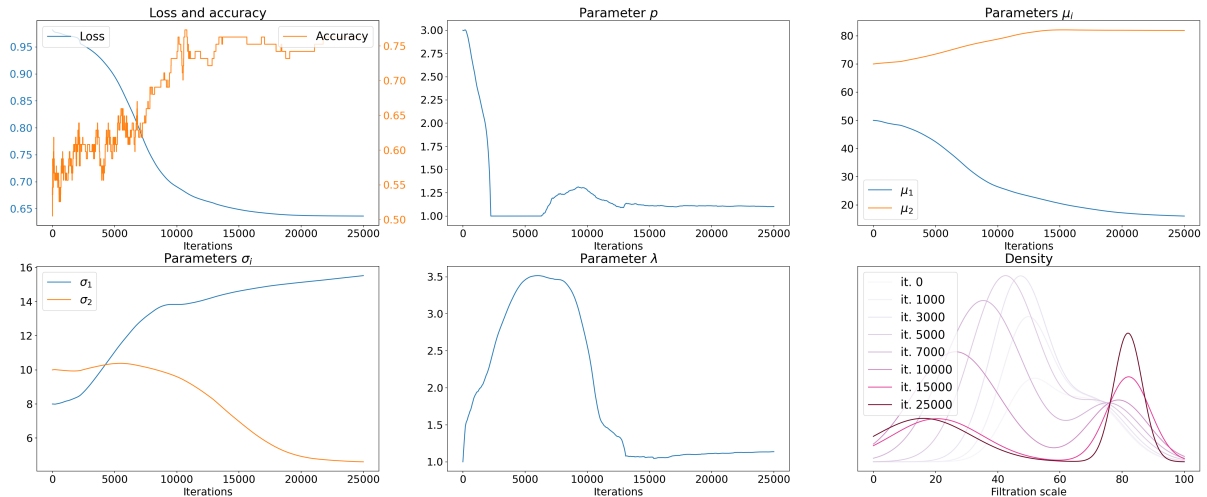


Figure 8: Results for one example run of the metric learning optimization for Wasserstein stable ranks (see Section 5.3) over 25000 iterations. **Top Left:** Progression of the loss and the KNN training fold accuracy over the iterations. **Top Middle, Top Right, Bottom Left, Bottom Middle:** Progression of the parameters in $\theta = (\mu_1, \mu_2, \sigma_1, \sigma_2, \lambda_2, p)$ parametrizing Wasserstein stable ranks: p , mean μ_i , standard deviation σ_i and λ_2 respectively over the iterations. **Bottom Right:** Density at different iterations.

p	μ_1	μ_2	σ_1	σ_2	λ
1.10 ± 0.04	16.45 ± 0.75	81.88 ± 0.27	15.51 ± 0.45	4.55 ± 0.24	1.15 ± 0.05

Table 1: Converged values for the parameters of the metric learning problem (mean and standard deviation over the LOOCV folds).

accuracy of 76.3% corresponding to the parameters that the optimization converged to, which we summarize in Table 1. This is an improvement also compared to the results obtained when only varying p and considering the standard contour in Figure 7. It is thus when we learn both p and the contour that the best loss and corresponding classification accuracy is achieved.

In Figure 9 we illustrate the effect of the metric learning by plotting the hierarchical clustering (with average linkage) corresponding to the standard stable ranks (i.e., with $p = \infty$ and standard contour) and to the optimized stable ranks. We see that the optimized stable ranks (with the exception of two outliers) group into two clusters: one with a majority of class A and the other with a majority of class B, while the pattern for standard stable ranks is less clear.

The optimal parameters found with the metric learning method are of interest because they allow to construct a distance space in which machine learning methods can be carried out, but they are also interpretable: they contain information about which features of the dataset are important to distinguish the two classes.

This is illustrated in Figure 10 where two sample barcodes – one from each class – are displayed with the optimal density superposed and the bars colored according to the density. From the insight that some parts of the filtration scale are more important in distinguishing younger from older subjects, one may pursue the analysis by looking for characteristics of bars in that region of the barcode. One can also take the analysis a step further by looking at the object from which the filtered simplicial complex was created. In our case, since the filtration

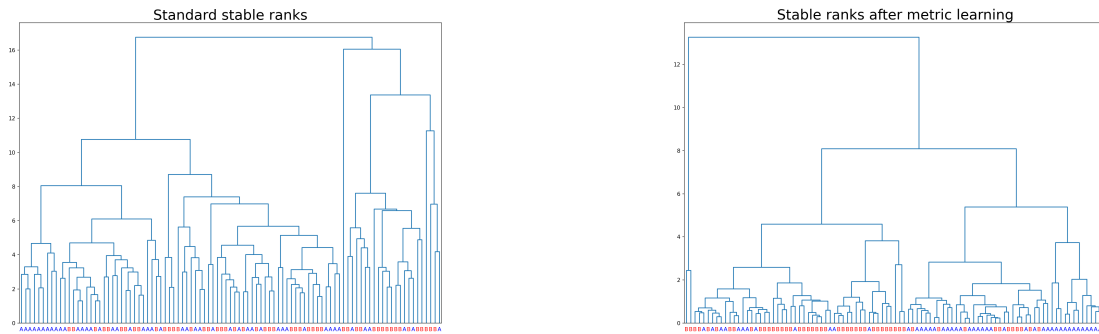


Figure 9: Hierarchical clustering on the standard stable ranks (left) and the optimized stable ranks resulting from the metric learning problem (right) with respect to the interleaving distance. The leaves (stable ranks in the dataset) are labeled and colored according to their class (A is $age \geq 45$, B is $age < 45$).

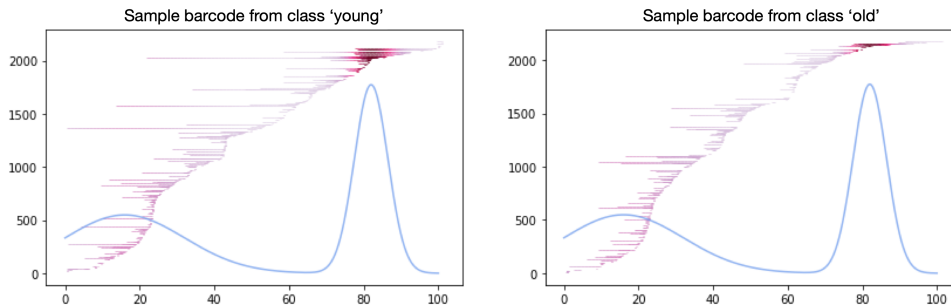


Figure 10: Sample barcodes from the two classes with superposed learned density. Bars are colored according to the density.

scale corresponds to the height (z -coordinate) in the 3D-embedding of the brain artery tree, one may for example investigate whether differences in brain artery between subjects of different ages in this particular region carries a biological meaning.

Acknowledgements

This work was partially supported by the Swedish Research Council (Vetenskapsrådet), the Wallenberg AI, Autonomous Systems and Software Program (WASP) funded by the Knut and Alice Wallenberg Foundation, the dBrain collaborative project at Digital Futures at KTH, the Strategic Support grant of the Digitalisation Platform at KTH, and by the Data Driven Life Science (DDLs) program funded by the Knut and Alice Wallenberg Foundation.

References

- [AEK⁺17] Henry Adams, Tegan Emerson, Michael Kirby, Rachel Neville, Chris Peterson, Patrick Shipman, Sofya Chepushtanova, Eric Hanson, Francis Motta, and Lori Ziegelmeier. Persistence images: A stable vector representation of persistent homology. *Journal of Machine Learning Research*, 18, 2017.

- [AM21] Henry Adams and Michael Moy. Topology applied to machine learning: from global to local. *Frontiers in Artificial Intelligence*, 4(668302), 2021.
- [ARSC21] Jens Agerberg, Ryan Ramanujam, Martina Scolamiero, and Wojciech Chachólski. Supervised learning using homology stable rank kernels. *Frontiers in Applied Mathematics and Statistics*, 7, 2021.
- [BDSS15] Peter Bubenik, Vin De Silva, and Jonathan Scott. Metrics for generalized persistence modules. *Foundations of Computational Mathematics*, 15(6):1501–1531, 2015.
- [BL15] Ulrich Bauer and Michael Lesnick. Induced matchings and the algebraic stability of persistence barcodes. *Journal of Computational Geometry*, 6(2):162–191, 2015.
- [BM21] Peter Bubenik and Nikola Milićević. Homological algebra for persistence modules. *Foundations of Computational Mathematics*, 21(5):1233–1278, 2021.
- [BMM⁺16] Paul Bendich, James S Marron, Ezra Miller, Alex Pieloch, and Sean Skwerer. Persistent homology analysis of brain artery trees. *The annals of applied statistics*, 10(1):198, 2016.
- [BS23] Ulrich Bauer and Maximilian Schmahl. Lifespan functors and natural dualities in persistent homology. *Homology, Homotopy and Applications*, 25(2):297–327, 2023.
- [BSS23] Peter Bubenik, Jonathan Scott, and Donald Stanley. Exact weights, path metrics, and algebraic Wasserstein distances. *Journal of Applied and Computational Topology*, 7(2):185–219, 2023.
- [BZM⁺10] Elizabeth Bullitt, Donglin Zeng, Benedicte Mortamet, Arpita Ghosh, Stephen R Aylward, Weili Lin, Bonita L Marks, and Keith Smith. The effects of healthy aging on intracerebral blood vessels visualized by magnetic resonance angiography. *Neurobiology of aging*, 31(2):290–300, 2010.
- [CCI⁺20] Mathieu Carrière, Frédéric Chazal, Yuichi Ike, Théo Lacombe, Martin Royer, and Yuhei Umeda. Perslay: A neural network layer for persistence diagrams and new graph topological signatures. In *International Conference on Artificial Intelligence and Statistics*, pages 2786–2796. PMLR, 2020.
- [CDSGO16] Frédéric Chazal, Vin De Silva, Marc Glisse, and Steve Oudot. *The structure and stability of persistence modules*, volume 10. Springer, 2016.
- [CGS22] Oliver A Chubet, Kirk P Gardner, and Donald R Sheehy. A theory of sub-barcodes. *arXiv preprint arXiv:2206.10504v1*, 2022.
- [CHLS18] Yu-Min Chung, Chuan-Shen Hu, Austin Lawson, and Clifford Smyth. Topological approaches to skin disease image analysis. In *2018 IEEE International Conference on Big Data (Big Data)*, pages 100–105. IEEE, 2018.

- [CR20] Wojciech Chachólski and Henri Riihimaki. Metrics and stabilization in one parameter persistence. *SIAM Journal on Applied Algebra and Geometry*, 4(1):69–98, 2020.
- [CSEHM10] David Cohen-Steiner, Herbert Edelsbrunner, John Harer, and Yuriy Mileyko. Lipschitz functions have L_p -stable persistence. *Foundations of computational mathematics*, 10(2):127–139, 2010.
- [CSEM06] David Cohen-Steiner, Herbert Edelsbrunner, and Dmitriy Morozov. Vines and vineyards by updating persistence in linear time. In *Proceedings of the twenty-second annual symposium on Computational geometry*, pages 119–126, 2006.
- [CWRW15] Yen-Chi Chen, Daren Wang, Alessandro Rinaldo, and Larry Wasserman. Statistical analysis of persistence intensity functions. *arXiv preprint arXiv:1510.02502v1*, 2015.
- [dSMS18] Vin de Silva, Elizabeth Munch, and Anastasios Stefanou. Theory of interleavings on categories with a flow. *Theory and Applications of Categories*, 33(21):583–607, 2018.
- [ELZ00] Herbert Edelsbrunner, David Letscher, and Afra Zomorodian. Topological persistence and simplification. In *Proceedings 41st annual symposium on foundations of computer science*, pages 454–463. IEEE, 2000.
- [Gäv18] Oliver Gävfert. Topology-based metric learning. *Conference poster. Available: https://people.kth.se/~oliverg/TAGS_poster.pdf*, 2018.
- [GC17] Oliver Gävfert and Wojciech Chachólski. Stable invariants for multidimensional persistence. *arXiv preprint arXiv:1703.03632v3*, 2017.
- [GHMM19] Kathryn Garside, Robin Henderson, Irina Makarenko, and Cristina Masoller. Topological data analysis of high resolution diabetic retinopathy images. *PloS one*, 14(5):e0217413, 2019.
- [GHS87] Gene H Golub, Alan Hoffman, and Gilbert W Stewart. A generalization of the eckart-young-mirsky matrix approximation theorem. *Linear Algebra and its applications*, 88:317–327, 1987.
- [GNOW21] Barbara Giunti, John S Nolan, Nina Otter, and Lukas Waas. Amplitudes in abelian categories. *arXiv preprint arXiv:2107.09036v4*, 2021.
- [GT19] Adélie Garin and Guillaume Tauzin. A topological “reading” lesson: Classification of MNIST using TDA. In *2019 18th IEEE International Conference On Machine Learning And Applications (ICMLA)*, pages 1551–1556. IEEE, 2019.
- [HKNU17] Christoph Hofer, Roland Kwitt, Marc Niethammer, and Andreas Uhl. Deep learning with topological signatures. *Advances in neural information processing systems*, 30, 2017.

- [H^{NH}+16] Yasuaki Hiraoka, Takenobu Nakamura, Akihiko Hirata, Emerson G Escolar, Kaname Matsue, and Yasumasa Nishiura. Hierarchical structures of amorphous solids characterized by persistent homology. *Proceedings of the National Academy of Sciences*, 113(26):7035–7040, 2016.
- [KFH17] Genki Kusano, Kenji Fukumizu, and Yasuaki Hiraoka. Kernel method for persistence diagrams via kernel embedding and weight factor. *The Journal of Machine Learning Research*, 18(1):6947–6987, 2017.
- [KMN17] Michael Kerber, Dmitriy Morozov, and Arnur Nigmatov. Geometry helps to compare persistence diagrams. *ACM Journal of Experimental Algorithmics*, 22(1.4):1–20, 2017.
- [Les15] Michael Lesnick. The theory of the interleaving distance on multidimensional persistence modules. *Foundations of Computational Mathematics*, 15(3):613–650, 2015.
- [Mil20] Ezra Miller. Essential graded algebra over polynomial rings with real exponents. *arXiv preprint arXiv:2008.03819v1*, 2020.
- [OPT⁺17] Nina Otter, Mason A Porter, Ulrike Tillmann, Peter Grindrod, and Heather A Harrington. A roadmap for the computation of persistent homology. *EPJ Data Science*, 6:1–38, 2017.
- [PGM⁺19] Adam Paszke, Sam Gross, Francisco Massa, Adam Lerer, James Bradbury, Gregory Chanan, Trevor Killeen, Zeming Lin, Natalia Gimelshein, Luca Antiga, et al. Pytorch: An imperative style, high-performance deep learning library. *Advances in neural information processing systems*, 32, 2019.
- [PVG⁺11] Fabian Pedregosa, Gaël Varoquaux, Alexandre Gramfort, Vincent Michel, Bertrand Thirion, Olivier Grisel, Mathieu Blondel, Peter Prettenhofer, Ron Weiss, Vincent Dubourg, et al. Scikit-learn: Machine learning in python. *The Journal of Machine Learning Research*, 12:2825–2830, 2011.
- [QTT⁺19] Talha Qaiser, Yee-Wah Tsang, Daiki Taniyama, Naoya Sakamoto, Kazuaki Nakane, David Epstein, and Nasir Rajpoot. Fast and accurate tumor segmentation of histology images using persistent homology and deep convolutional features. *Medical image analysis*, 55:1–14, 2019.
- [RCB21] Raphael Reinauer, Matteo Caorsi, and Nicolas Berkouk. Persformer: A transformer architecture for topological machine learning. *arXiv preprint arXiv:2112.15210v2*, 2021.
- [RHBK15] Jan Reininghaus, Stefan Huber, Ulrich Bauer, and Roland Kwitt. A stable multi-scale kernel for topological machine learning. In *Proceedings of the IEEE conference on computer vision and pattern recognition*, pages 4741–4748, 2015.
- [Rot09] Joseph Rotman. *An Introduction to Homological Algebra*. Springer-Verlag New York, 2nd edition, 2009.

- [SCL⁺17] Martina Scalamiero, Wojciech Chachólski, Anders Lundman, Ryan Ramanujam, and Sebastian Öberg. Multidimensional persistence and noise. *Foundations of Computational Mathematics*, 17(6):1367–1406, 2017.
- [SHP17] Bernadette J Stolz, Heather A Harrington, and Mason A Porter. Persistent homology of time-dependent functional networks constructed from coupled time series. *Chaos: An Interdisciplinary Journal of Nonlinear Science*, 27(4):047410, 2017.
- [ST20] Primoz Skraba and Katharine Turner. Wasserstein stability for persistence diagrams. *arXiv preprint arXiv:2006.16824v5*, 2020.
- [Ste04] J Michael Steele. *The Cauchy-Schwarz master class: an introduction to the art of mathematical inequalities*. Cambridge University Press, 2004.
- [TNVL21] Renata Turkeš, Jannes Nys, Tim Verdonck, and Steven Latré. Noise robustness of persistent homology on greyscale images, across filtrations and signatures. *PloS one*, 16(9):e0257215, 2021.
- [Vin90] A Vince. A rearrangement inequality and the permutahedron. *The American mathematical monthly*, 97(4):319–323, 1990.
- [ZC05] Afra Zomorodian and Gunnar Carlsson. Computing persistent homology. *Discrete & Computational Geometry*, 33:249–274, 2005.
- [ZW19] Qi Zhao and Yusu Wang. Learning metrics for persistence-based summaries and applications for graph classification. *Advances in Neural Information Processing Systems*, 32, 2019.

DEPARTMENT OF MATHEMATICS, KTH, S-10044 STOCKHOLM, SWEDEN

{jensag,guidolin,isaacren,scola}@kth.se

Corresponding author: Martina Scalamiero (scola@kth.se)